UNIVERSITY OF CALIFORNIA
RIVERSIDE

Synthesis and Processing of Nanocrystalline Aluminum Nitride

A Thesis submitted in partial satisfaction
of the requirements for the degree of

Master of Science

in

Materials Science and Engineering

by

Matthew Albert Duarte

August 2016

Thesis Committee:
Dr. Javier E. Garay, Chairperson
Dr. Yasuhiro Kodera
Dr. Masaru Rao

The Thesis of Matthew Albert Duarte is approved:

_____

_____

_____

Committee Chairperson

University of California, Riverside

Acknowledgements

I would like to dedicate this work to my mother, Irene Duarte for always supporting me unconditionally, my brothers, Richard and Dennis Duarte for constantly reminding me to not stray from the path I chose to follow. And finally to my close friends that stuck with me through this adventure.

I thank the guidance and support of my advisors, Dr. Javier Garay and Dr. Yasuhiro Kodera. Dr. Kodera's contributions to the project were invaluable, especially in to complete the bulk of my work. Also, without the many knowledgeable members of AMPS Lab – Kyle Chan, Alexander Dupuy, Darren Dewitt, Anthony Fong, Nikte Gomez, Corey Hardin, Elias Penilla, Pathikumar Sellappan, Meir Shachar, Gottlieb Uahengo, Aleksey Volodchenkov, Chad Warren and Andrew Wieg – the completion of my research and studies would not have been possible.

Furthermore, the help of my undergraduate researcher, Christian Niño, in completing much of the building projects necessary for research was invaluable.

ABSTRACT OF THE THESIS

Synthesis and Processing of Nanocrystalline Aluminum Nitride

by

Matthew Albert Duarte

Master of Science, Graduate Program in Materials Science and Engineering
University of California, Riverside, August 2016
Dr. Javier E. Garay, Chairperson

Synthesis, processing and characterization of nanocrystalline aluminum nitride has been systematically studied due to the material's unique properties. Through a controllable and tunable processing method utilizing gas nitridation for the purpose of reducing/nitriding nanocrystalline γ-alumina, yielding a grain size of ~80 nm. Single phase aluminum nitride powder was obtained at temperatures of 1100°C – 1400°C. Further processing of AlN powders was performed by CAPAD (Current Activated Pressure Assisted Densification) to obtain dense single phase aluminum nitride. Dense bulk aluminum nitride was obtained at temperatures as low as 1300°C. The composition of the single phase aluminum nitride was evaluated by characterization methods such as X-Ray diffraction and photoluminescence.

Table of Contents

List of Figures

Chapter 1 Introduction and Motivation

1.1 Nanocrystalline Materials

Nano means one billionth, measurements at this level is in nanometers (nm) – billionth of a meter 1^{-9} m. Nanocrystalline materials refers to the materials in the form of thin films, nano particles, nanotubes, nanowires, anything with at least one dimensional length being less than 100 nm [1] . In recent years, nanotechnology has grown exponentially, as shown in Figure 1.1.

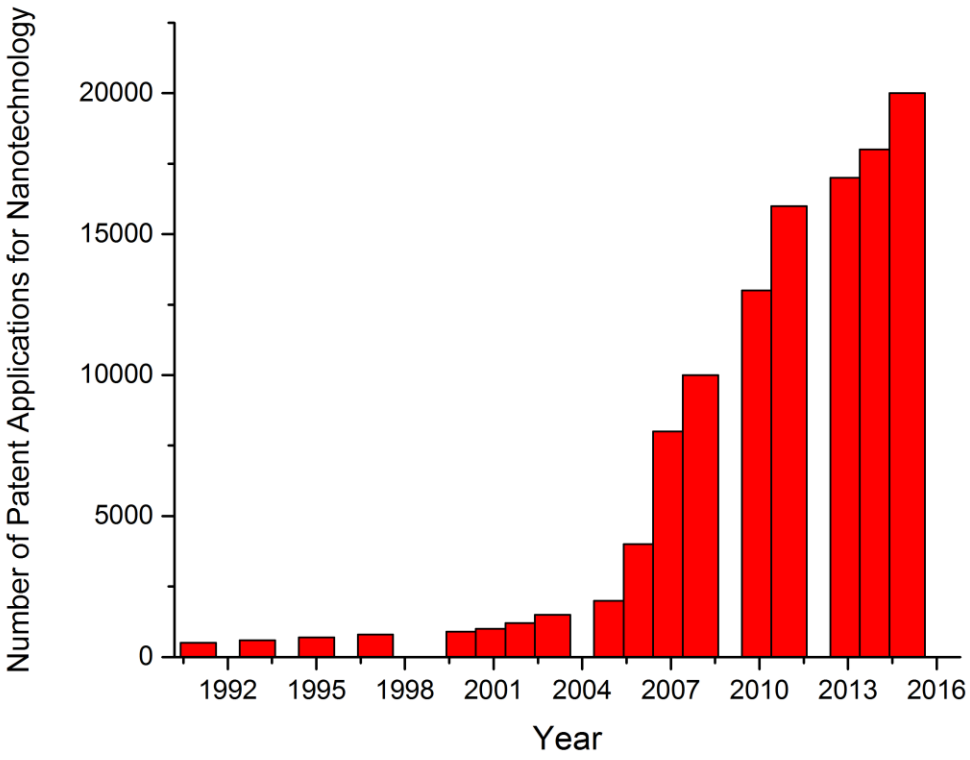

Figure 1.1 Representation of accelerated technology growth.

The large scale attention to nanocrystalline materials is the possibility it creates for nanotechnology, for its structures to have novel properties. Due to the small sizes, nanotechnology builds on the ability to control or manipulate objects at the atomic scale. Properties of materials are size-dependent in this scale range. Thus, when particle size is made to be nanoscale, properties such as melting point, fluorescence, electrical conductivity, magnetic permeability, and chemical reactivity change as a function of the size of the particle.

1.2 Aim of this Study

The aim of this study was to develop a process to, produce nanocrystalline aluminum nitride in the forms of powders and 3D bulk materials, and characterize them. By synthesizing nanocrystalline aluminum nitride through the reduction/nitridation of γ-Al_2O_3, the end product may have improved the thermal, optical, electrical, and mechanical properties. The properties have been studied and explored very well in single crystal and polycrystalline micron-sized aluminum nitride. These properties have not been studied very well in nanocrystalline bulk aluminum nitride. The following work will describe the processing methods for the synthesis of nanocrystalline aluminum nitride powders and 3D bulk materials.

Chapter 2 Background

2.1 Aluminum Nitride

Aluminum nitride, AlN, is a ceramic with a useful set of thermal and electrical properties. Among these properties are high thermal conductivity, low coefficient of thermal expansion, excellent dielectric properties, nontoxicity, and high temperature resistance [2]. The price for aluminum nitride is more than that of alumina, which is used for many substrate and dielectric applications. Alumina, however, cannot meet the requirements for many high-brightness LED and power electronics applications. AlN is one of the few ceramics that features an interesting combination of very high thermal conductivity and excellent electrical insulation properties [2]. Because of this, aluminum nitride is used in many industrial applications such as, opto-electronics, and electronic substrates, where the need for high thermal conductivity is necessary.

2.2 Aluminum Oxide

Alumina, aluminum oxide (Al_2O_3), is present in many different polymorphs and crystal structures. Its uses in our daily lives are prominent, used in tooth pastes, porcelain bathtubs, spark plugs, tires and catalytic converters in cars. The excellent stoichiometry and stability of Al_2O_3 help to make it an important component of many protective oxides that can be formed on the surface of high-temperature metals [1]. Most importantly of all, aluminum oxide was used as an aluminum precursor for the synthesis of aluminum nitride which is the main interest and purpose of this study.

Aluminum oxide exists in many metastable polymorphs besides the only thermodynamically stable α-Al_2O_3. The metastable Al_2O_3 structures are divided into two broad categories: a face-centered cubic (fcc) or a hexagonal close-packed (hcp) arrangement of oxygen anions. It is the distribution of cations within each subgroup that results in the different polymorphs. The Al_2O_3 structures based on fcc packing of oxygen include γ, η(cubic), θ (monoclinic), and δ (either tetragonal or orthorhombic), whereas the Al_2O_3 structures based on hcp packing are represented by the α (trigonal), κ (orthorhombic), and χ (hexagonal) phases [1].

Metastable Al_2O_3 phases are synthesized by many different processing methods. Differences in the phase transformation sequence are mainly attributed to the different structures the precursor material has [1].

All transition aluminas phases are reproducible and remain stable at room temperature, but the sequence of transformations is not reversible when the temperature decreases after the point of transformation. α- alumina is the only stable phase having a high melting point, and high thermal stability [1].

γ- and η-Al2O3 have been described as defect spinel structures. It is sometimes useful to describe the spinel as a layered structure on the {111} planes. The packing of the {111} oxygen anion layers forms an ABCABC sequence, whereas the packing of the aluminum cations can be described by two types of alternating layers: either (i) layers containing only octahedrally coordinated cations or (ii) ‘‘mixed’’ layers containing both octahedrally and tetrahedrally coordinated cations [1].

2.2.1 Structure of Aluminum Nitride

Aluminum nitride is mostly a covalent material, ca. 75% and crystallizes under the wurtzite structure a=3.111 Å and c=4.978 Å, c/a=1.600Å with the space group of $P6_3mc$, that is, hexagonal close packing of the anions with the cations filling half of the tetrahedral sites. The unit cell contains two anions, one at the origin and on the inside of the cell, as shown in Figure 2.2.2. Close packed layers occurs at the basal plane, where c=0 and c= ½ and therefore that stacking sequence is hexagonal, ABABA. This crystal structure can be distorted into a variety of polytypes with the addition of impurity elements [3].

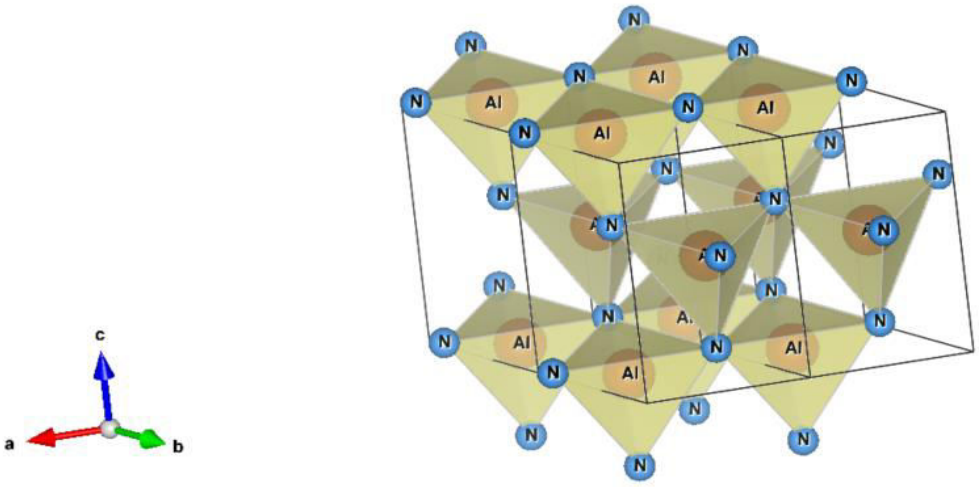

Figure 2.2.1. Aluminum Nitride wurtzite structure generated via VESTA Software. [4]

2.2.3 Properties of Aluminum Nitride

The properties of interest to us are the hardness and thermal conductivity of the material. Both these properties are fundamental to having a functional ceramic for miniaturization or high power outputs in thermal management applications.

Hardness

Hardness is a measure of how resistant solid matter is to various kinds of permanent shape change when a compressive force is applied. Some materials, such as metal, are harder than others. The Mohs scale of mineral hardness is a qualitative ordinal scale that characterizes the scratch resistance of various minerals through the ability of a harder material to scratch a softer material. Macroscopic hardness is generally characterized by strong intermolecular bonds, but the behavior of solid materials under force is complex [5]. Hardness is important, since it is related to a number of other important properties or performance aspects of ceramics including compressive strength, wear, erosion, machinability, and ballistic performance. Of microstructure factors, grain size dependence of hardness (H) is particularly important since low or zero porosity is required and obtained in many cases, making porosity effects less critical [5].

It has commonly been accepted that hardness generally increases with decreasing grain size, in metals and some ceramics, due to the Hall-Petch type effects on the associated plastic flow. [6] Therefore, it is in our interest to see whether aluminum nitride would behave in the same manner.

Hardness values on the Mohs scale ranging from 5 to between 9 and 10 are found in the literature for aluminum nitride. Results varied somewhat with the direction, probably because of the anisotropic nature of the crystals. The over-all hardness of aluminum nitride appears to be 7 on the Mohs scale [7]. **With the**

Thermal Conductivity

Heat moves through a material at a specific rate. The rate it travels depends on the material itself. Thermal conductivity is a material property describing the ability to conduct heat. Thermal conductivity is the material property of most interest when talking about aluminum nitride.

In general two carrier types can contribute to thermal conductivity, electrons and phonons. In nanostructures phonons usually dominate and the phonon properties of the structure become of a particular importance for thermal conductivity. These phonon properties include: phonon group velocity, phonon scattering mechanisms and heat capacity [8].

Polycrystalline ceramics exhibit lower thermal conductivities than their associated single crystals. For instance, at 300K, the theoretical thermal conductivity of single crystal aluminum nitride (AlN) is 319 W/m-K, whereas, the values measured for polycrystalline AlN ceramics range from 17 W/m-K to 285 W/m-K at room temperature [9].This variation is not unusual for polycrystalline ceramics. The variability is strongly dependent upon the purity of the starting materials and the details of sintering process.

The process is important since it influences the microstructure and thus influences the conduction mechanism [9].

Unlike typical ceramics, AlN has low atomic mass, simple crystal structure, strong interatomic forces, and low phonon scattering which makes it intrinsically thermally conductive. It is based upon such knowledge that Slack [9]developed rules for identification of crystals with high thermal conductivity, i.e., the crystal should have (1) low atomic mass (2) strong bonding and (3) simple crystal structure. Aluminum nitride has a low atomic mass, it is a covalently bonded material, and has a relatively simple crystal structure, that of hexagonal crystal structure [9].

However, thermal conductivity of polycrystalline sintered AlN is influenced by microstructure; secondary phases, including porosity; impurities, such as oxygen and other cationic impurities; and processing-related factors. Achieving good thermal conductivity and dielectric properties is directly related to processing. Similar to any other ceramic material, good control of process depends directly on properties of the raw materials. This particularly is true of AlN because impurity content and microstructure, which influence thermal conductivity, directly depend on quality of the starting powders that will be reacted to synthesize AlN [2].

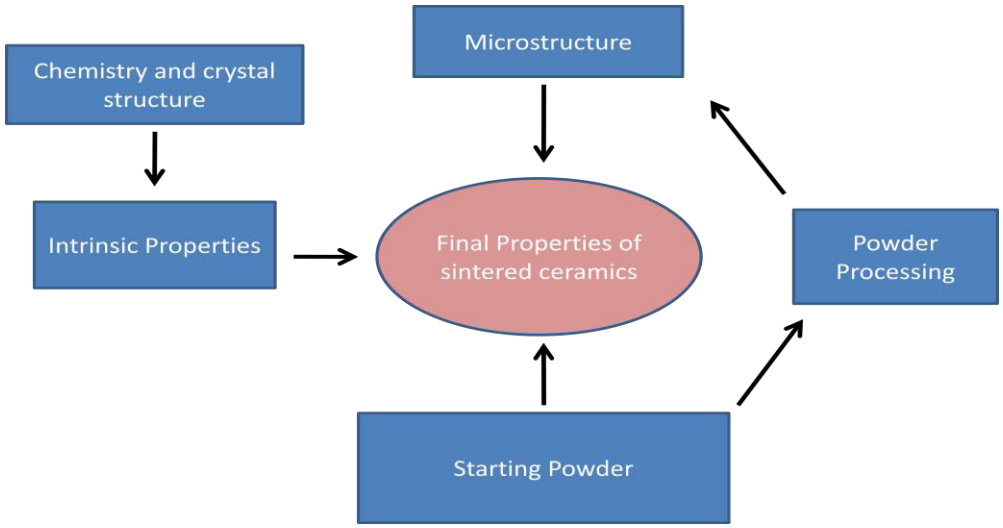

Figure 2.2.3 Processing routes and methods that affect final properties of ceramics.

2.3 Processing of Aluminum Nitride

Aluminum nitride ceramic processing begins with powder synthesis. Properties of the starting powder, including purity, particle-size distribution and morphology, surface area, and bulk densities dictate processing approaches, such as densification. Aluminum nitride powder can be synthesized via various approaches. However, direct nitridation and carbothermal reduction and nitridation are the two most widely used routes for producing aluminum nitride powder in tonnage-scale quantities. Each offers advantages and disadvantages [2].

2.3.1 Direct Nitridation

Aluminum nitride can be synthesized from aluminum metal and nitrogen gas via the direct nitridation process which is a self-propagating exothermic reaction.

$$2Al\ (s\ or\ l) + N_2(g) \rightarrow 2AlN(s) + \ heat \quad (2.3.1)$$

The direct nitridation, DN, process typically involves ignition of aluminum powders in a nitrogen containing atmosphere. Reacted product requires further processing via milling or classification to produce final powders. The advantages of direct nitridation synthesis are its energy efficiency and environmental friendliness. The exothermic reaction generates ~328 kJ/mol at 1,800 K. Aluminum melts at 933 K and the reaction with nitrogen begins at ~1,073 K, making it a self-sustaining process. Other than the initial ignition, which does not require much energy, no additional external heat is needed to sustain the reaction, making the process extremely energy efficient [2].

The disadvantages of this process are milling is required to obtain a final product and the possibilities of impurities. Uncontrollable reaction sequence and exothermic temperature induce considerable necking between aluminum nitride particles, resulting in agglomeration that is difficult to break up during milling. Consequently, multiple particle size reduction steps are necessary to achieve required particle sizes. These milling steps can introduce potential impurities depending on milling media and milling conditions [2].

2.3.2 Carbothermal Reduction and Nitridation

Typical precursors are aluminum oxide powders mixed with a source of carbon as a reducing agent. The precursors are combined and heat treated at 1,400°C–1,800°C in the presence of nitrogen or nitrogen-containing gas [2]. The overall reaction is

$$Al_2O_3\ (s) + 3C\ (s) + N_2\ (g) + heat \rightarrow 2AlN\ (s) + 3CO\ (g) \qquad (2.3.2)$$

Theoretically, the reaction needs three moles of carbon for every mole of Al_2O_3. However, practical issues, such as surface area and mixing limitations, require a substantial amount of excess carbon (~15%–30% additional carbon) to promote full conversion to AlN. The advantages of carbothermal reduction and nitridation,CRN, synthesis are the quality of the powder and minimal or no milling required. For the most part, precursor particle size and synthesis temperature determine final particle size and purity levels of CRN powders. Finer particle size is possible without excessive milling because of availability of fine precursor powders [2].

The disadvantages of this process are the high cost, the energy intensive requirements and the carbon footprint/environmental impact. Expensive precursors and energy-intensive multiple heat treatment steps makes this powder very expensive compared with DN powders. Powder cost may not be a big factor in some advanced applications, such as growing single crystals for UV-LEDs, phosphors, and advanced microelectronic packaging [2]. However, for applications such as HB-LEDs, CRN powders are simply unaffordable. Production of high purity Al_2O_3 powders is itself an energy intensive process requiring initial conversion of ore to metal and then purified

metal into oxide. Added to that are the reduction and nitridation heat-treatment steps. Typically, synthesis occurs at temperatures well above 1,400°C and approaching 1,800°C, usually in graphite furnaces. Calcination is necessary to burn off excess carbon after synthesis [2].

In addition to the carbon emissions that result from energy required for several heat-treatment steps, the reaction itself produces a significant amount of carbon (in the form of CO and CO_2) as a byproduct. For every 100 g of AlN, the reaction produces ~160 g of CO_2 — not counting the excess carbon needed from practical considerations for complete conversion of Al_2O_3 to AlN. The common perception that CRN powders provide better properties for thermal management applications may not be justified. A brief literature review and considerable hands-on experience suggest that powder synthesis method has little impact on the final properties, including thermal conductivity of the sintered product [2].

What matters are properties of the AlN powder, such as purity, crystallinity, and particle size and distribution. Carefully engineered DN powders should perform as well or better than CRN powders as long as the powder properties are matched. It is admittedly more challenging to achieve finer particle size and high purity by DN, but, by using proper high-purity, fine-particle-size, large-surface-area aluminum precursor powders and closely controlling synthesis reaction rate and subsequent milling, high quality DN AlN powder can be made economically in tonnage quantities [2].

2.3.3 Non Carbon Gas Nitriding

In gas nitriding the donor is a nitrogen rich gas, usually ammonia. When ammonia comes into contact with the surface, it dissociates into nitrogen and hydrogen. The nitrogen then diffuses into the surface of the material creating a nitride layer. Unfortunately, for ammonia to fully dissociate, high temperatures must be reached >1100°C. The gas nitriding process also requires a long period of time [more explanation]. The layer usually consists of two zones – the compound layer (white layer) which can be a cubic or hexagonal nitride and the diffusion layer below with dissolved and hard nitride precipitates [10].

2.3.4 Processing of γ-Alumina by Gas Nitridation

γ-Al_2O_3 is a good starting material to produce nanocrystalline aluminum nitride because of its fine particle size, high surface area and reactivity. The overall reaction can be explained by

$$Al_2O_3 + 2NH_3 \rightarrow 2AlN + 3H_2O \quad (2.3.4)$$

However, synthesis of aluminum nitride from γ-Al2O3 nanoparticles requires relatively high temperatures and a reactive gas, ammonia or nitrogen.

Previous work has included conversion of $Al(OH)_3$ into AlN powder under a gas mixture of C_3H_8 and NH_3 at a reaction temperature of 1200°C. Their interest in using that gas mixture was the propane increased the reactivity of $Al(OH)_3$ which can lower the

reaction temperature. Also, $Al(OH)_3$ demonstrated to be a highly reactive starting material in comparison to α-Al_2O_3 [11].

Kroke used several kinds of aluminum oxide precursors including $Al(OH)_3$ as starting materials, and reported that the aluminum oxide precursors reacted with NH_3 atmospheres at 1000–1400◦C to form single-phase AlN with crystallites of 5–60 nm [12]. Because of this, there is an interest in developing a process to fully convert nanocrystalline AlN at lower temperatures.

However, there is a challenge in synthesizing nanocrystalline AlN from γ-Al2O3. (1) Nano sized powder has high surface energies, so in order to lower that energy, it will form agglomerates making it difficult to keep powder nanosized. (2) Synthesis of AlN requires temperatures over 1100°C and grain growth is extremely dominant at those temperatures. (3) Aluminum nitride readily wants to have oxygen, to form alpha alumina a more stable compound.

Since γ-Al2O3 is a fine powder, with nano grains, the particles will readily agglomerate into large clusters. High surface area to volume ratio of nanoparticles provides a very high surface energy. To minimize its surface energy the nanoparticles create agglomeration. Uncontrolled agglomeration of nanoparticles many occur due to attractive Van Der Waals forces between particles. With smaller size, higher relative surface area, and higher relative numbers of surface atoms there is higher surface energy. Such surface atoms have unsaturated coordinations (not complete coordination) and each atom has vacant coordination sites. A phenomenon so called dangling bonds. More bonds

need to be formed per each surface atom. They try to make bonds, and such bonds tend to form between adjacent particles (bonds between surface atoms of each), this causes agglomeration [13].

Agglomeration has shown significant influences on the sintering process and compaction in experiments. The sintered density of powders decreased with increasing agglomeration strength. Agglomerates limits attainable green body density, interferes with the development of microstructure, impeded initial-stage sintering kinetics and limited the potential benefit of fine crystallites in final-stage sintering. These agglomerates will result in large crack-like voids or pores due to differential sintering [13].

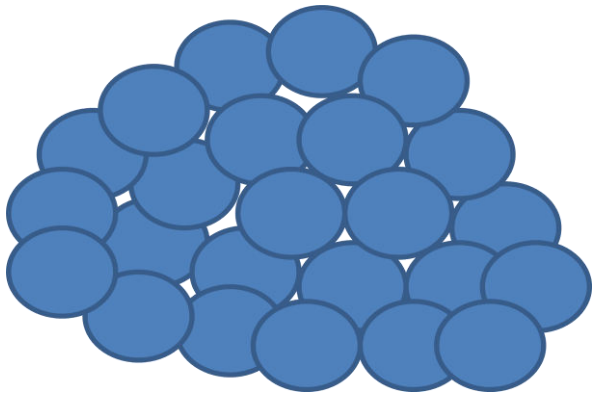

Figure 2.3.4 Nanoparticles readily form agglomerates into clusters.

Since synthesis of AlN powder requires temperatures greater than 1100°C, the difficulty then lies with keeping the nanoparticles from sintering as they are processed in the tube furnace. At such high temperatures, grain growth becomes significant on the order of sub-micron, making further processing troublesome as grains are expected to

grow. Another difficulty in synthesizing aluminum nitride powder is that aluminum has a strong affinity to bond with oxygen, more so than nitrogen, in order to form alpha alumina which is a more stable compound.

2.4 CAPAD Processing

Current Activated Pressure Assisted Densification, CAPAD, is a process which relies on a high current to induce joule heating while simultaneously applying a load pressure to allow for rapid sintering of powders all while under vacuum levels to the 10^{-3} Torr. Densification of powders is dependent on both thermodynamics and kinetics, therefore, temperature, time and pressure are the primary parameters in attaining high density. By utilizing rapid joule heating, at heating rates ranging from 100-600°C/minute, to reach densification temperatures while simultaneously apply a load pressure (50-500 MPa). With CAPAD, it is possible to reach densities of 95-99% in minutes rather than the several hours necessary in traditional sintering processes [14].

The advantages of densifying materials through CAPAD are especially evident when dealing with optical materials and intermediate/metaphase phases. With optical materials, trace amounts of pores, imperfections, inclusions and other defects act as photon scattering sites. Therefore optical materials require high density and purity. While purity of the material usually occurs at the powder preparation level, the ability to reach fully density in minimal time through CAPAD processing allows for the elimination of porosity while preserving grain size and structure, thereby creating ideal optical materials [14]. Another advantage of CAPAD processing is the ability to control and overcome

thermodynamic instability or the preservation of metastable phases. Typically, metastable phases cannot exist under normal processing conditions due to the time and temperature dependence of material phases [15]. However, with CAPAD processing, it is possible to preserve metastable phases in bulk forms.

2.4.1 CAPAD System and Sample Preparation

The CAPAD system used in all powder processing consists of two copper electrodes with graphite spacers acting as the actual heating and pressure contact on the samples, as shown in Figure 2.4.1. Load forces of up to [600kN] are applied by an Instron 5500 series load cell. The graphite spacers and samples are enclosed within a water-cooled vacuum chamber to prevent oxidation reactions during processing. Typical experiments were conducted with temperature monitored through either a thermocouple (at 1200°C or below) or a pyrometer (above 1000°C) [14].

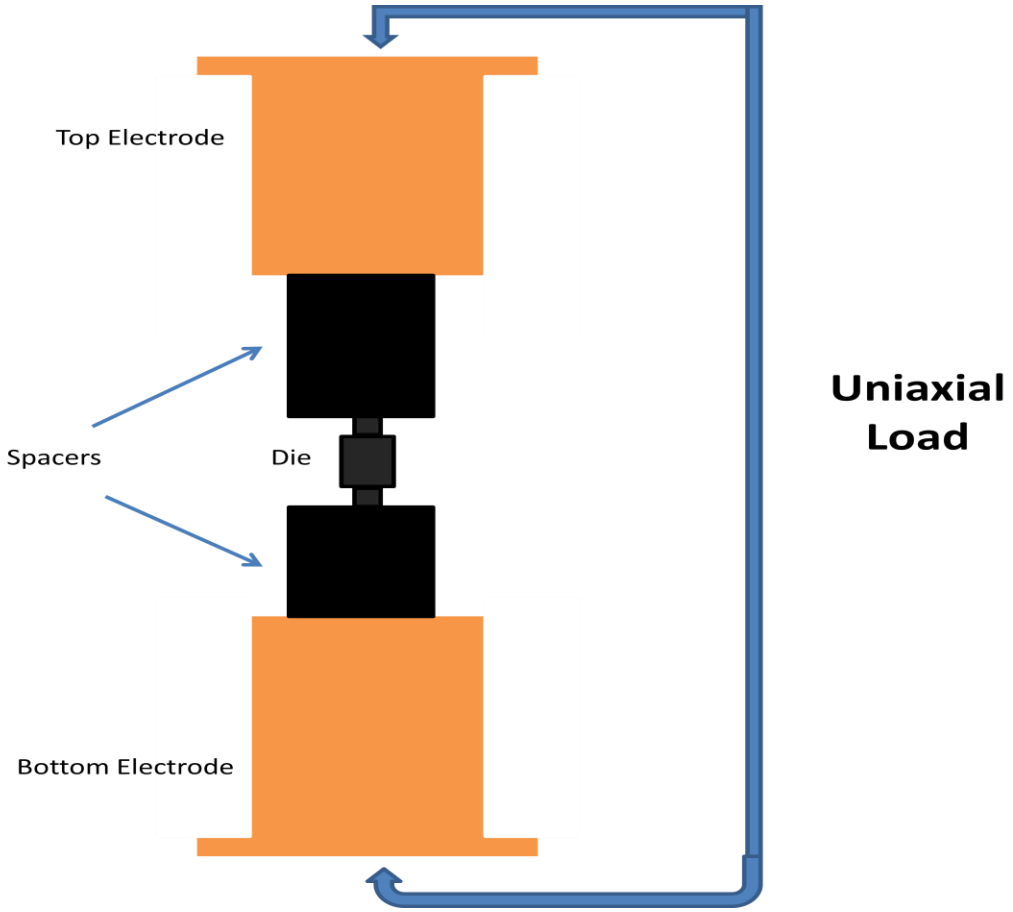

Figure 2.4.1 Schematic of CAPAD system.

Sample powders were prepared using a two-part graphite die/plunger setup. In order to minimize powder usage and to increase homogeneity of densified samples, powder was placed within a miniature graphite die of 5mm inner diameter and 20mm outer diameter, and pressed between two 10mm miniature plungers. The smaller die and plunger set was then inserted into a larger graphite die with 20mm inner diameter, and pressed between two larger 20mm diameter diffuser plungers [14].

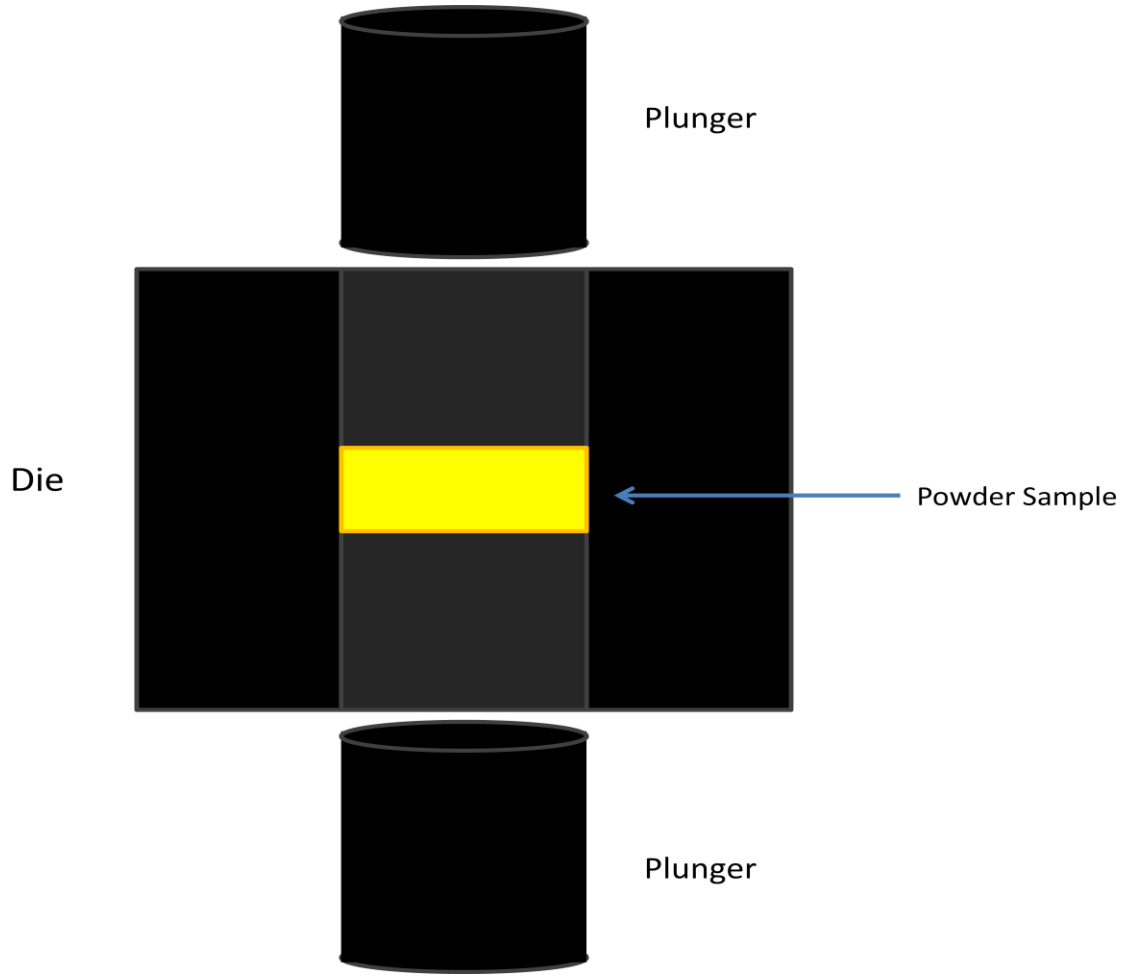

Figure 2.4.1.2 Schematic of Die System used in CAPAD Processing.

2.4.2 Solid-State Densification

It is generally accepted that the reduction in the surface free energy of a compact, due to the elimination of internal surface area associated with the pores, provides the driving force for densification. When compared to other processes, e.g. chemical reactions, the decrease in the surface free energy during densification is rather small, ~100J/mol for particles with an initial diameter of 1um, but the distance the matter has to

be transported is also small (of the order of the particles sizes), so that densification occurs at a reasonable rate at sufficiently high temperatures [16].

The specific energy and curvature of the particles provides an effective stress on the atoms under the surface. For a curved surface with radii of curvature r_1 and r_2, this stress is given by the equation of Young and Laplace:

$$\sigma = \gamma_{sv}\left(\left(\frac{1}{r_1}\right) + \left(\frac{1}{r_2}\right)\right) \qquad (2.4.2)$$

where the γ_{sv} is the specific surface energy. The diffusion potential, μ, which drives mass transport is in this case found by equating the mechanical work performed by the stress to the thermodynamics work required for the reduction of the surface free energy. A commonly used relation is

$$\mu = \sigma\Omega \qquad (2.4.2.1)$$

where Ω is the atomic or molar volume. The equation for μ is actually more complex for polycrystalline ceramics where the pores are in contact with the grain boundaries [16]. For example, in the final stage of densification where the pores are assumed to be spherical, one expression is [18]:

$$\mu = \Omega\left(\left(\frac{2\gamma_{gb}}{G}\right) + \left(\frac{2\gamma_{sv}}{r}\right)\right) \qquad (2.4.2.2)$$

where γ_{gb} is the specific energy of the grain boundary, G is the diameter of the grains, and r is the radius of the pores. According to equation 2.4.2.2, the chemical potential consists of two contributions, one attributed t the pores and the other attributed to the boundaries [16].

2.4.3 Stages of Densification

The microstructure of a powder compact, consisting initially of discrete particles, evolves continuously during densification. However, it is sometimes convenient to divide the process into three idealized stages defined in terms of the microstructure, to force correspondence between simple, established densification models [16].

The initial stage would begin as soon as some degree of atomic mobility is achieved and during this stage, sharply concave necks form between the individual particles. The amount of densification is small, typically the first 5% of linear shrinkage, and it can be considerably lower if coarsening mechanisms are very active. In the intermediate stage, the high curvatures of the initial stage have been moderated and the microstructure consists of a three-dimensional interpenetrating network of solid particles and continuous, channel-like pores [16]. This stage is considered valid to ~5-10% and therefore covers most of the densification. Grain growth starts to become significant at this stage. As densification proceeds, the channel-like pores break down into isolated, closed voids, which marks the start of the final stage. Grain growth can be more extensive in the final stage and difficulties are commonly encountered in the removal of the last few percent of porosity [16].

2.4.4. Mechanisms for Densification

Densification of crystalline materials can occur by several mechanisms, i.e. atomic transport paths, surface diffusion, lattice diffusion, grain boundary diffusion, and dislocation motion. Figure 2.4 shows a schematic representation of the mass transport paths for two particles. A distinction is commonly made between densifying and non-

densifying mechanisms. Surface diffusion and lattice diffusion from the particles surfaces to the neck lead to neck growth and coarsening of the particles without densification [16]. Grain boundary diffusion and lattice diffusion from the grain boundary to the neck are the most important densifying mechanisms in polycrystalline ceramics. Diffusion from the grain boundaries to the pores permits neck growth as well as densification [16].

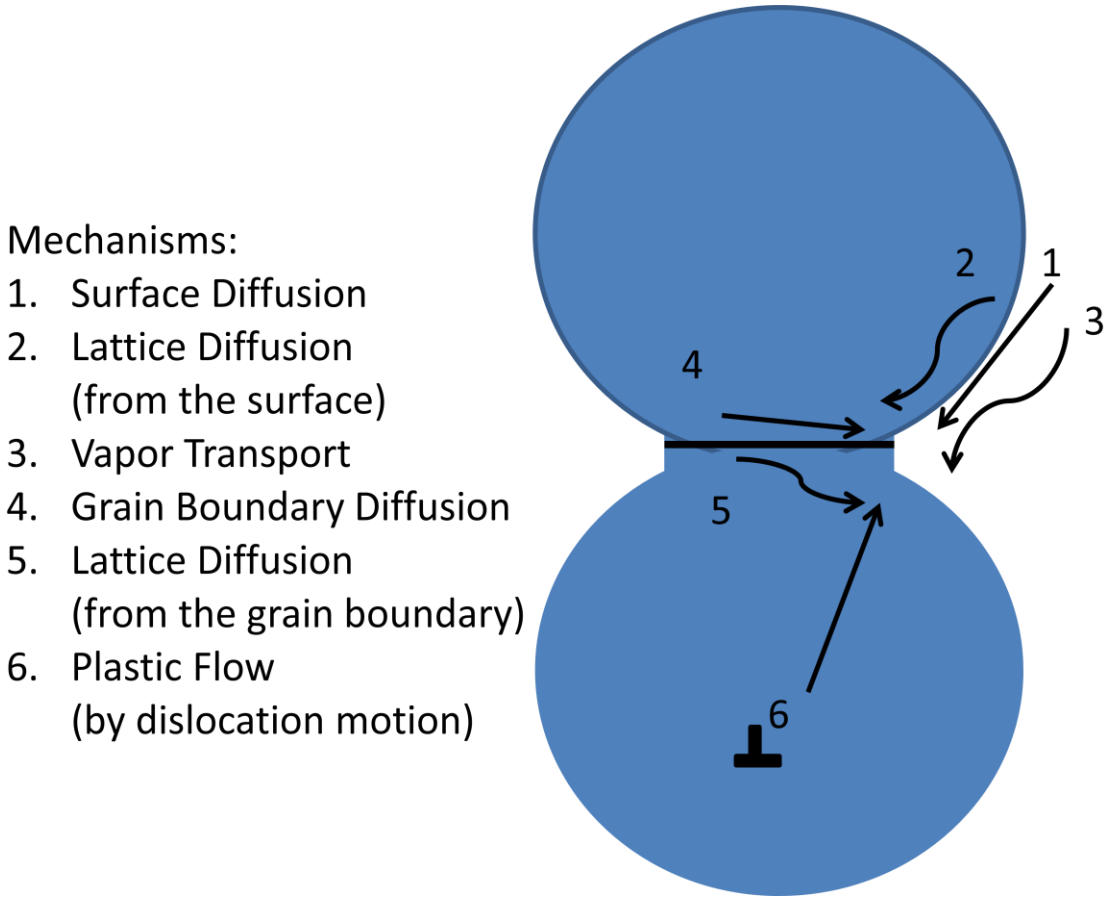

Figure 2.4 Densifying mechanisms between polycrystalline particles.

2.5 Applications of AlN Bulk

AlN is an ideal material for applications needing electrical insulation and thermal conductivity. Constantly growing demand for miniaturization, long life, and high performance in the electronics and semiconductor industries for packaging, power electronics, inverters for transportation, telecommunications, cooling systems, high-brightness LEDs, and more make AlN a very attractive material [2].

Chapter 3 Materials and Methods

Based on the idea of reactive gas nitridation, nanocrystalline aluminum nitride powder was obtained. By nitriding the γ-alumina powder at different temperatures, atmospheric environment and times, AlN powder with different compositions and sizes were obtained, studied and discussed.

3.1 Materials

Starting materials to prepare nanocrystalline aluminum nitride powder is the aluminum precursor, γ-Al2O3, from Aframat Advanced Materials, 99.9% purity, starting grain size ~40 nm. Nitrogen and ammonia used in this study was produced by Air Gas Company with nitrogen purity of 99.9% and 99.5% ammonia purity.

3.2 Experimental Procedure

Fine pure gamma alumina powder was placed in an alumina boat. The mass of the powder placed ranged from 0.30 to 1.50 grams.

Reactions were carried out in a horizontal alumina tube heated by a furnace as shown in Figure 3.2. The reaction tube was heated at room temperature and the nitrogen and ammonia was introduced to the tube during the heating period. When the tube reached temperature and was stably maintained, it was held at set temperature for a certain amount of time, then the temperature gradually decreased to room temperature while ammonia was continuously flowing. After transferring the sample to a glove box, the weight of the sample was measured.

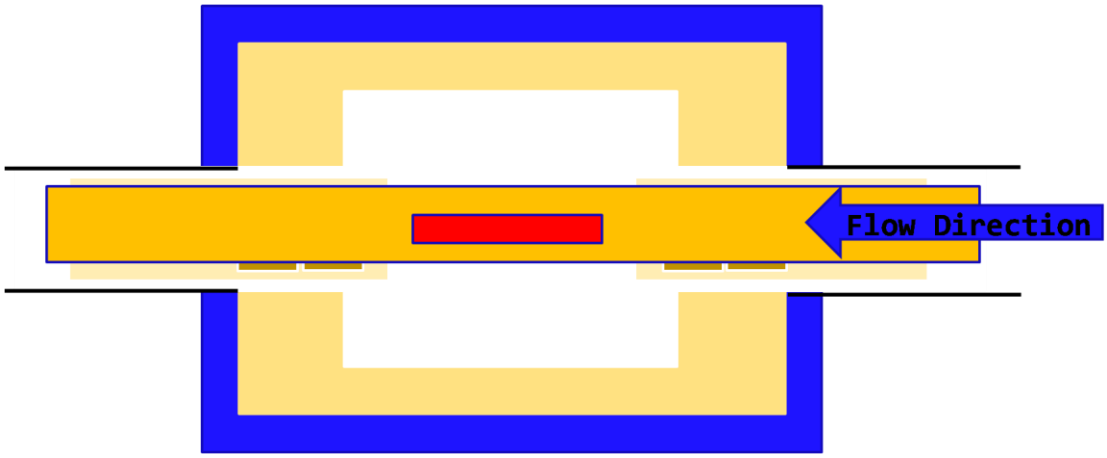

Figure 3.2 Schematic of horizontal tube furnace used in nitridation reactions.

In order to minimize powder usage and increase homogeneity of densified samples, aluminum nitride powder is prepared in a miniature graphite die and plunger set. The amount of powder used in each CAPAD run was 0.25 grams. Samples were taken to temperatures of 1100°C to 1600°C and held for 10 minutes under a load pressure of 105MPa. The heating rate of each experiment was approximately 500°C/min. After cooling the samples are then lightly polished as to remove any residual graphite on the surface of the bulk material.

3.3 Characterization Methods

Various characterization methods were used in this study. The following are some brief descriptions of the characterization methods. These characterization techniques were used on both the powder and bulk samples.

3.3.1. X-Ray Diffraction (XRD)

A widely used method of material characterization is X-Ray Diffraction, XRD, and crystallography. All crystalline materials have unique combinations of the Bravais Lattices, and thus a unique combination of miller indices. An additional consequence of crystalline materials is that the atomic spacing is uniform throughout the materials, in the absence of structural defects and abnormalities, due to the repeating periodic arrangements of lattices. X-rays, being a form of electromagnetic radiation, interact with individual atoms within a crystal lattice in a wave-particle manner, resulting in some combination of absorption, reflection, and scattering, known collectively as diffraction [17]**.** Due to the wave-like nature of X-ray scattering, either constructive or destructive interference can occur. X-ray diffraction powder analysis techniques typically rely on the detection of constructive interference patterns, which can be explained through Bragg's Law:

$$2dsin\theta = n\lambda \qquad (3.3.1)$$

where n=1, 2, 3…is the order of constructive interference, λ is the wavelength of the incident x-ray, d is the planar spacing, and θ is the angle of incidence [17].The planar spacing combination, being unique to each material, can be calculated for cubic systems as

$$d = \frac{a}{h+k+l} \qquad (3.3.1.1)$$

where h, k, l are the integers denoting the miller indices which are planes orthogonal to a reciprocal lattice vector. Hexagonal and rhombohedral systems can have a fourth index number typically denoted as i, a redundant index in addition to the other miller indices

$$i = -(h + k) \qquad (3.3.1.2)$$

given these known parameters, it is possible to correlate constructive interference patterns from x-ray diffraction to specific crystallographic planes [18].

3.3.2 Scanning Electron Microscopy (SEM)

While X-ray diffraction is a useful characterization tool for determining crystal structure and phase, it is useful to have visual confirmation of particle morphology and grain size. Scanning Electron Microscopy, SEM, is a tool used for surface morphology and grain size characterization of both powder and bulk samples ranging from 10 nm to several 100 μm [19].

In SEM, an electron beam is typically generated either by thermionic electron emission, or field electron emission. Thermionic electron emission guns are comprised of both a cathode and an anode, with a filament (usually tungsten or lanthanum hexaboride) acting as the cathode, is heated to the point which electrons are energized to the point where they are able to overcome the work function energy of a material, and escape into a vacuum toward the anode [19].

In SEM, due to the energetic behavior of electrons, multiple emissions can be generated from an electron beam interacting with a sample. These emissions include unscattered electrons, inelastically scattered electrons, elastically scattered electrons, absorbed electrons, backscattered electrons, secondary electrons, X-rays, auger electrons and light (UV, visible or infrared). Under most circumstances, SEM detectors utilize either secondary electrons or backscattered electrons to generate maps [20].

Chapter 4 Results and Discussion

In this chapter, the main results of this study are summarized. Nanocrystalline aluminum nitride powders in the morphologies of nanoparticles were synthesized and characterized. Bulk aluminum nitride was also processed and characterized.

4.1 Optimizing Synthesis of Nanocrystalline Aluminum Nitride

When placing the γ-alumina powder on the alumina boat, the initial thought was that each position on the boat would nitride equally. Conversion, grain size and overall homogenity became a function of boat position. As shown in Figure 4.1.1, intial alumina boat positioning was a 15cm x 3cm (in green) with alumina powder placed 2 cm apart from each other. Through XRD, only positions 4 and 5 completely nitride. The other positions show a combination of α-alumina peaks along with AlN, as shown in Figure 4.1.2. All powders were processed at 1300°C for 1 hour.

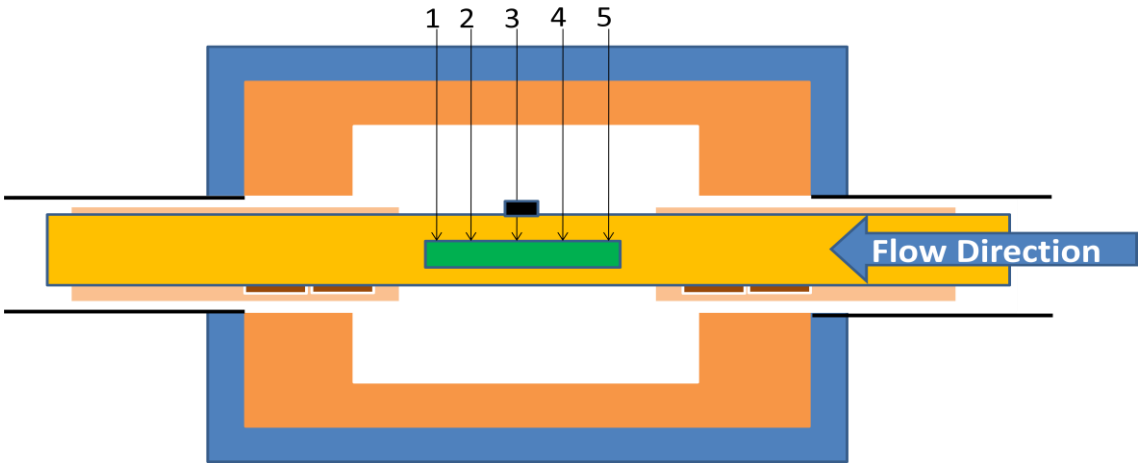

Figure 4.1.1. Schematic of tube furnace with alumina boat in green and different powder positions labeled.

The α-alumina peaks, (012) and the (113) at 26° and 43°, respectively, decrease as the position in the boat increases. The closer the powder is to the flowing end of the tube, the more converted that powder is to aluminum nitride. The reason for this might be that as the ammonia is initially hitting the alumina boat and powders, most of the reaction is taking place, leaving the remaining end of the tube to have less and less product even with a continuous flow. The XRD data, in Figure 4.1.2., shows the difference in conversion of aluminum nitride as the position of powders in the alumina boat changes.

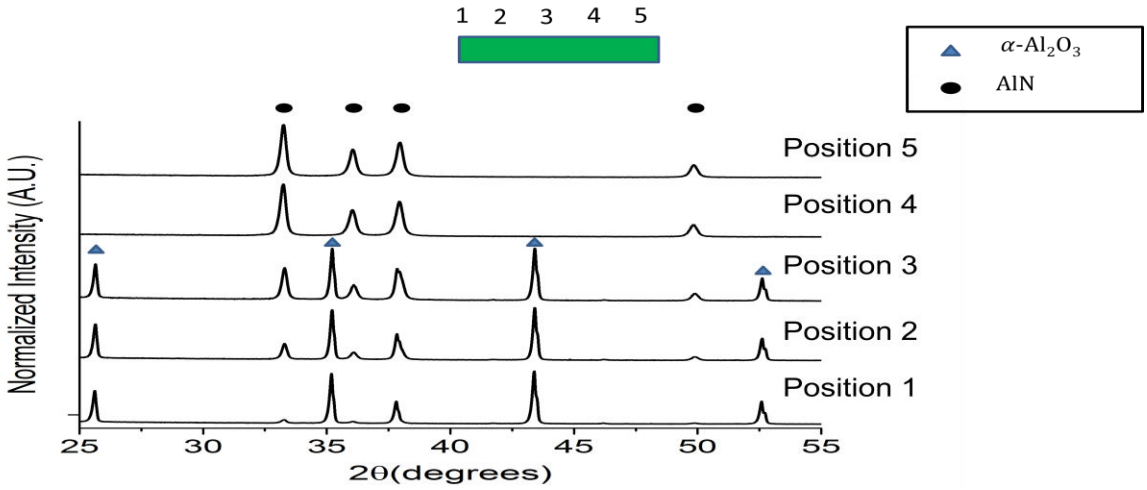

Figure 4.1.2. XRD data of aluminum nitride conversion being a function of powder position in an alumina boat.

This is a problem when considering the amount of powder yielded at the end of each processing run, less than 0.15 grams. A normal CAPAD experiment requires at least 0.25 grams. Also, XRD shows that there are inhomogenities between positions, so mixing positions 4 and 5, although both aluminum nitride, wouldn't be beneficial for futher use. The conversion of the alumina powder is affected on its location on the boat. With such a

small conversion region, approximately 5 cm, a new design had to be implemented, in order to ensure that there isn't a mixture of single phase aluminum nitride with a two phase powder system.

In order to solve the problem of getting a small region of conversion for the powders, a new design for an alumina boat was implemented. The alumina boat was replaced by using an 45cm alumina half pipe. The powder was spaced out by 3.8 cm and a larger amount of powder was placed in the pipe.

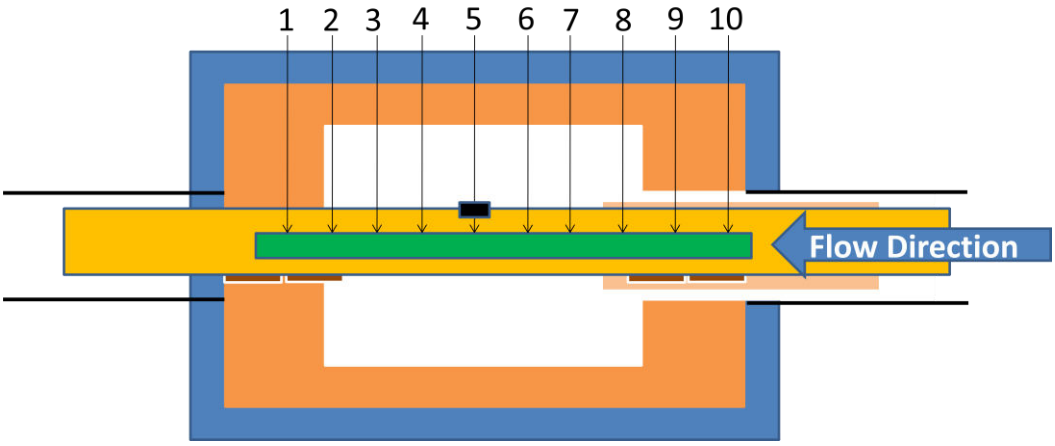

Figure 4.1.3. New Schematic of tube furnace with alumina boat, in red, and different powder positions labeled. The powder was spaced out by 3.8 cm from each position.

The phase composition as shown in XRD, in Figure 4.1.4., reveals the same gradient as the old setup. Positions 1-4, only position 1 and 4 are shown, show two alpha alumina peak the (012) at 26° and the (113) at 43°. The remaining positions 5-10, only

position 5 and 10 are shown, show single phase aluminum nitride with broader crystalline peaks with increasing position. Only data for 4 different positions were shown because it is assumed the behavior throughout the pipe will remain similar except at transitioning positions.

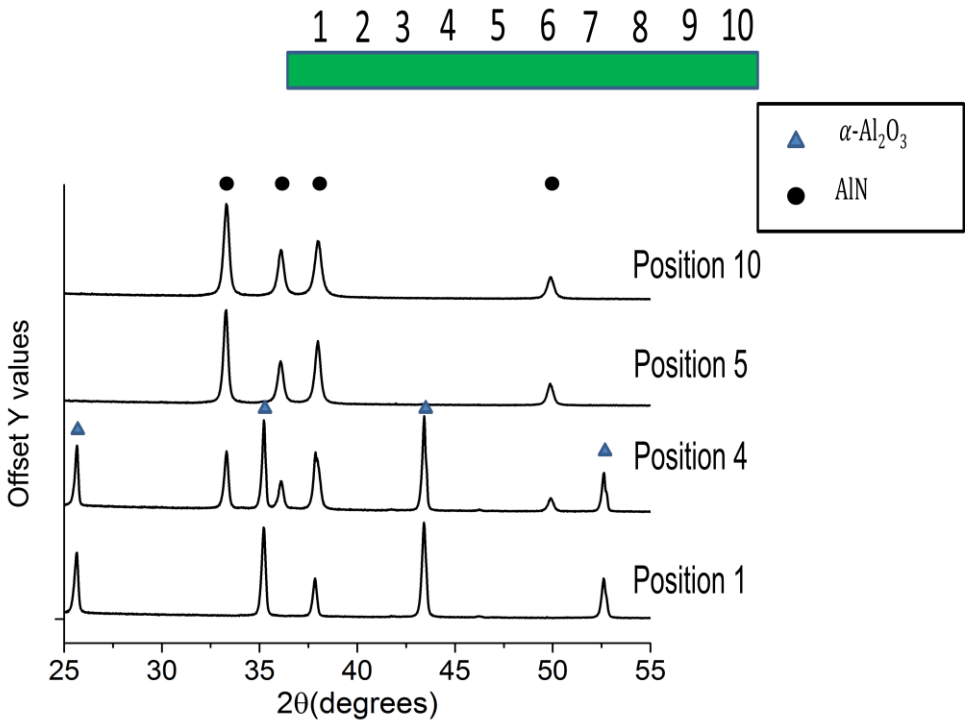

Figure 4.1.4. XRD data of aluminum nitride conversion being a function of powder position in an alumina boat.

With the new setup, the amount of powder after each run is ~ 1.5 grams, 10 times more than the previous setup. However, as with the previous setup, there is an inhomogeneity between powder positions. The amount of powder that can be used in CAPAD processing from this setup is approximately 0.60 grams.

With gradients being apparent in terms of tube length, the gradient of powder and tube height came into question. Powder is usually stacked on each other at each position having a height of approximately 3 cm. Having a height of powder while flowing ammonia into the tube is going to affect the reactivity of all the powder. Powder at the surface should convert more readily than powder at the bottom of the tube. As shown in Figure 4.1.5., XRD analysis confirms our suspicions. Powder was placed in position 10

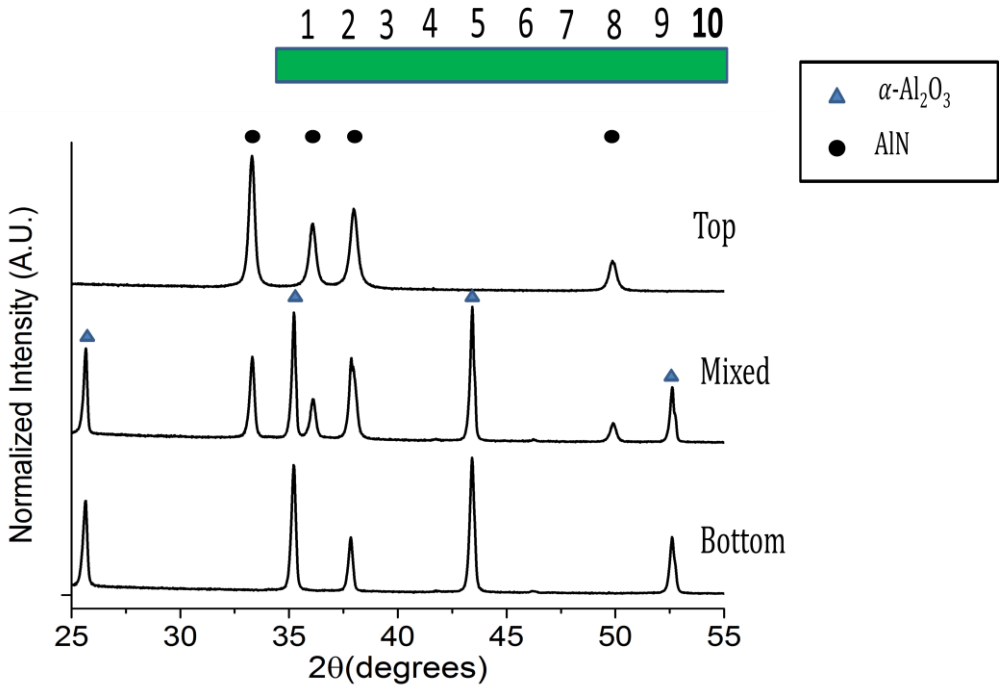

Figure 4.1.5. XRD analysis of aluminum nitride conversion in terms of height positioning

at 1300°C for 2 hours. The powder was taken by grabbing the top and bottom of the powder separately with tweezers, the rest of the powder was mixed to see the overall composition. Based from XRD analysis, the top of the powders show the 3 aluminum nitride peaks and the bottom and mixed powder revealed a mixture between α-alumina

and aluminum nitride. SEM images, Figure 4.1.6., show the effect that height positioning has on the grain growth of the powder. The top of the powder has significanty smaller grains in comparison to the powder at the bottom of the tube. The size of the grains at the bottom of the tube is approximately 0.7 μm.

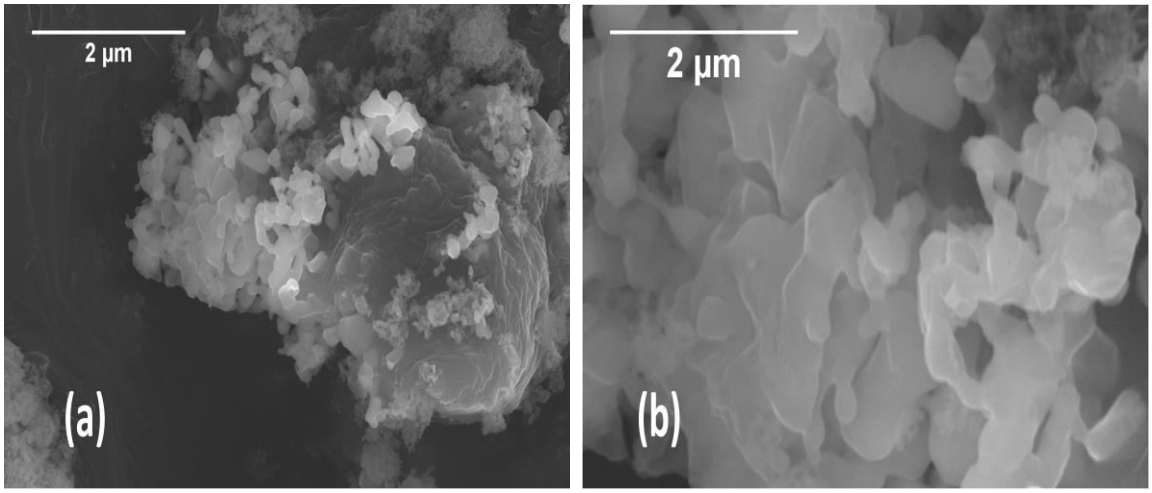

Figure 4.1.6. SEM images showing the effect of height positioning has on the grain growth of the powder, with (a) being the top of the powder and (b) being the bottom.

A visual representation of the conversion gradient occuring when there is a large disparity in the heights of the powder is shown in Figure 4.1.7. The yellow particles represent the powder being placed throughout the tube and the black line being the division where the conversion gradient will become apparent.

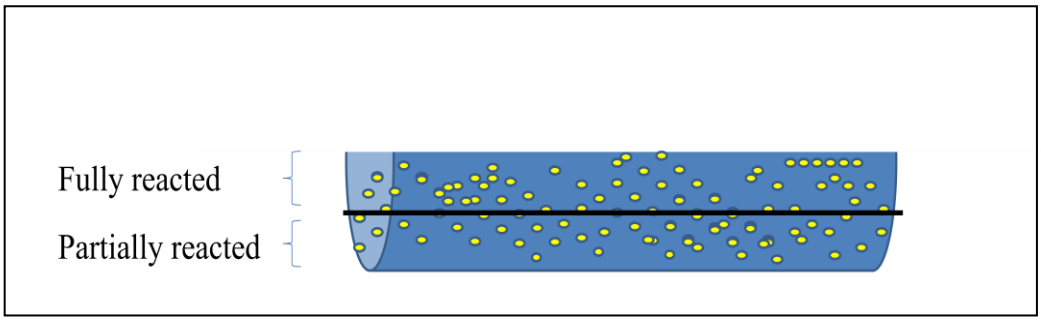

Figure 4.1.7. Schematic of the conversion gradient in terms of height positioning.

In order to solve this issue, the height of the powder was decreased to ~ 1 cm. This decreased the amount of powder that would yield for each run to 0.30 grams. This powder amount is enough for one CAPAD processing run, which is acceptable as it helps reduce any inhomogenieties there might be between a batch of powders.

The inhomogeniety in powder conversion as a function of position can be explained by the dissociation and decomposition ammonia undergoes as it travels through the tube funrnace. Upon initial contact of the powder, the ammonia reacts to with the alumina to form aluminum nitride, however, as the gas is already used of its reactants, doesn't provide the same level of reactivity with the powders placed in thepositions further down. Also, as mentioned in equation (2.3.4), one of the products of the reduction reaction is water. The presence of water will reduce the partial pressure in the overall tube and lower the reactivity that ammonia wil have on the remainder of the alumina powder.

So in order to optimize the synthesis of nanocrystalline nanocrystalline aluminum nitride, multiple processing parameters in the tube furnace had to be considered. For each processing run, a temperature of 1300°C was run for 2 hours. The best results in

nanocrystalline and conversion to aluminum nitride came from powders in position 9 and 10 having a powder height of ~1 cm. Each processing run yields enough powder for a single CAPAD run.

4.2 Synthesis of Nanocrystalline Aluminum Nitride

The nanocrystalline aluminum nitride powder was obtained at a relatively low temperature of 1200°C without the use of propane gas. The morphology and phase transformation of γ-alumina to AlN is discussed. The aluminum precursor, γ-alumina, had a starting grain size of approximately 40 nm. The powder, as shown in Figure 4.2.1, has numerous crystallites grouped, this can prove to be an issue in the reduction and nitridation process.

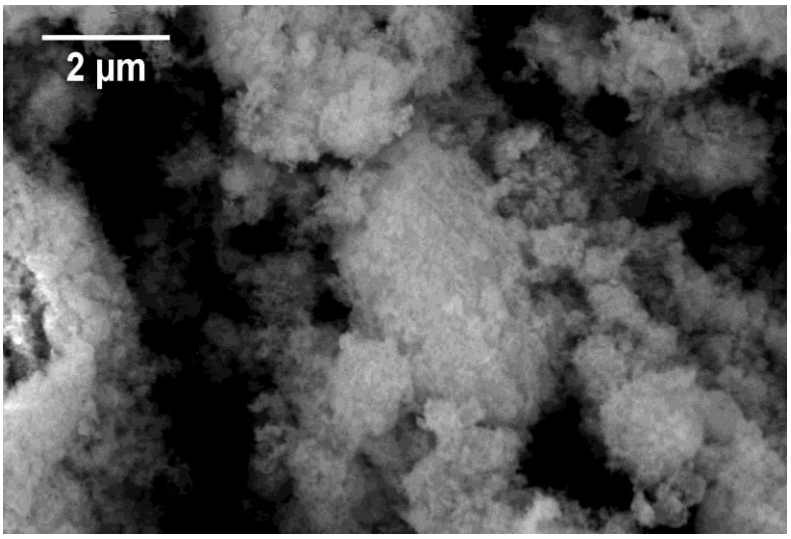

Figure 4.2.1 Unreacted y-alumina as received powder.

The overall experimental nitridation process is described in Figure 4.2.2. At 1100°C, the ammonia gas that is already introduced into the furnace begins to dissociate

into nitrogen and hydrogen. This is the nitrogen source at diffuses into the alumina and forming nitride layers while pulling out oxygen of the alumina to react with the hydrogen to form water molecules. The process reduces the alumina by introducing ammonia into the system to form aluminum nitride and water.

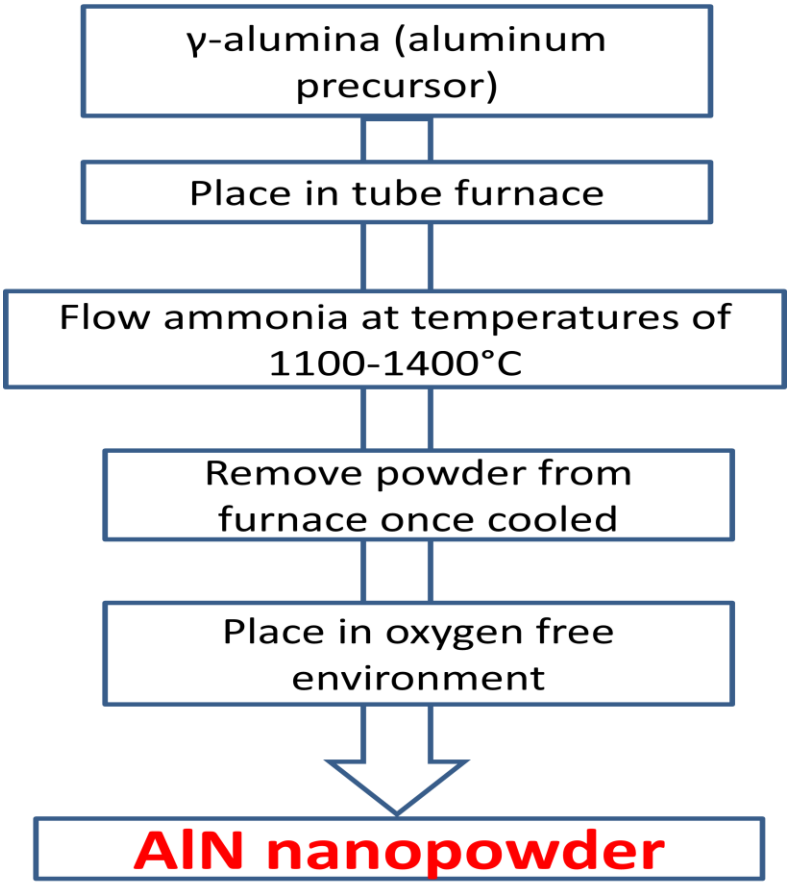

Figure 4.2.2. Flow chart describing process for nitridation.

When γ-alumina is processed in the tube furnace under different reaction temperatures, varying levels of nitridation of the alumina powder takes place. The higher the reaction temperature is, the higher the conversion rate will be. This conversion rate

can be briefly explained by the Gibb Free Energy of the system. Since the reaction is greatly dependent on the temperature, the [idea] is that the higher the overall reaction is the likely the final product will be converted. This is shown in XRD diffraction patterns in Figure 4.2.3.

The γ-alumina was processed in the tube furnace at temperatures of 1100 – 1400°C for a 1 hour hold. At a temperature ramp of 5°C/min, the tube was constantly being flowed with ammonia gas until the powder and tube cool down to room temperature.

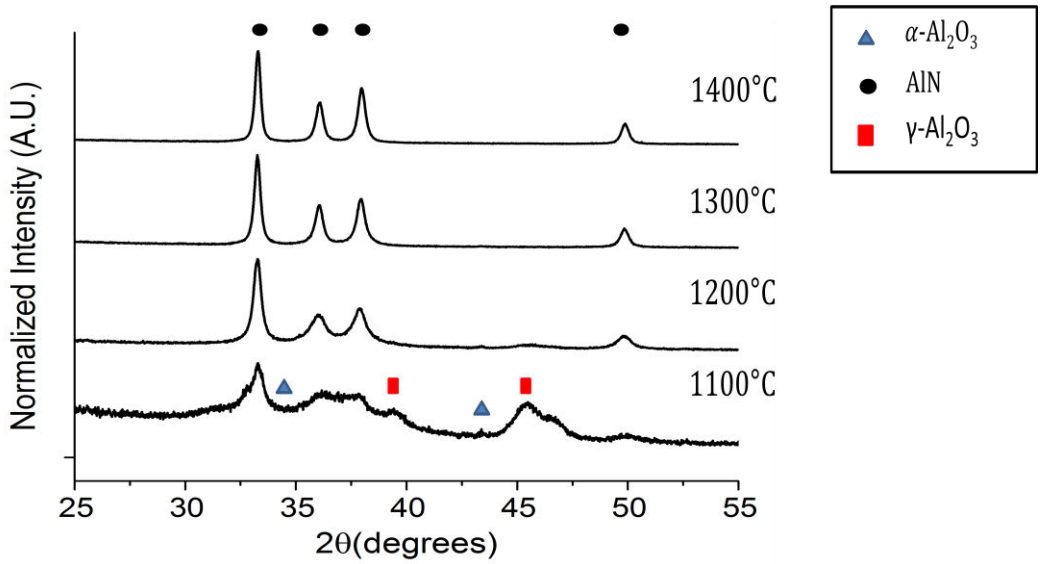

Figure 4.2.3. XRD diffraction patterns of γ-Al_2O_3 powders being processed at different temperatures for 1 hour.

At a temperature of 1100°C, the y-alumina powder is shows low crystallinity. It is comprised of two phases, a gamma-alumina phase and an aluminum nitride phase, when comparing between the ICSD database standard. At 1100°C, the powder is not fully converted and is transitioning into the aluminum nitride phase. Ammonia begins to

dissociate at 1100°C, indicating that conversion of the powder begins at low temperatures such as these. At temperatures higher than 1100°C, the conversion into aluminum nitride becomes more apparent. At 1200°C, the (220) peak at 46°, of γ-alumina is slightly shown. At temperatures above 1200°C, based on XRD analysis, full conversion to aluminum nitride has occurred. SEM images of the processed powders is shown in Figure 4.2.4. These images reveal, that as the temperatures that we are nitriding the powder increases there is an increase in the grain size.

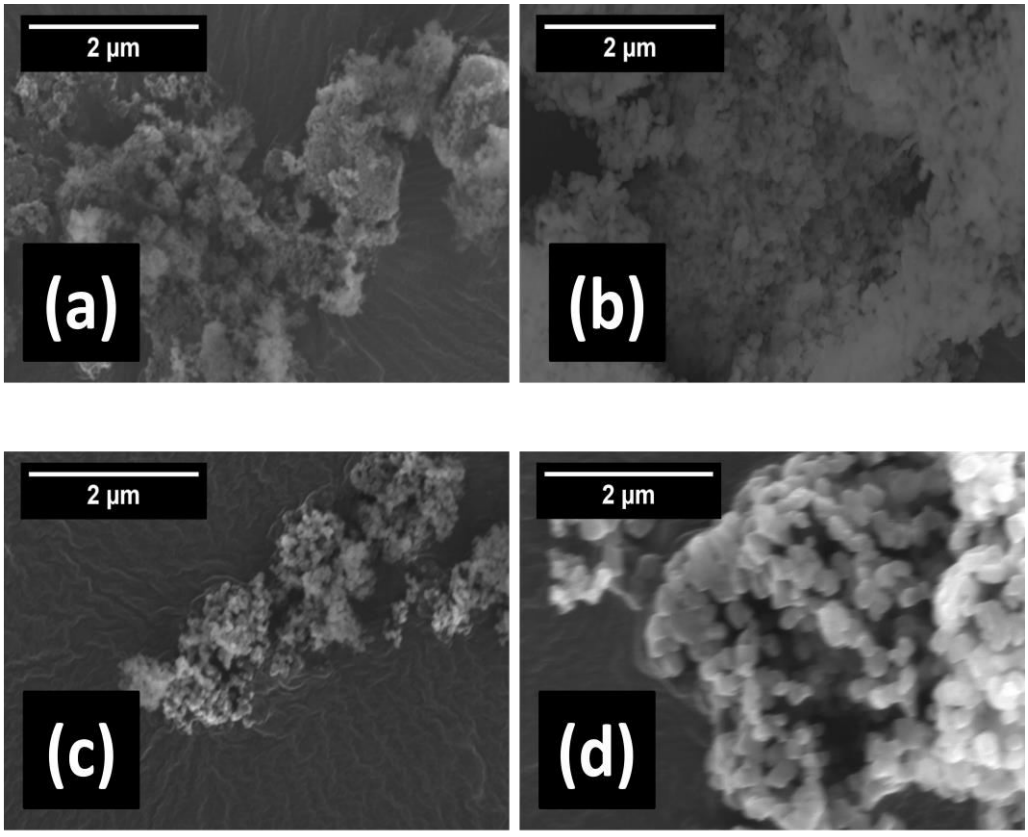

Figure 4.2.4. SEM images of powders processed at different temperatures in the tube furnace (b) 1100°C (c) 1200°C (d) 1300°C (e) 1400°C, for 1 hour each.

The trend occuring with the nitridation of γ-Al_2O_3 that is evident is that, as temperatures increases there is an increase in the conversion to aluminum nitride and the grain size grows significantly along with it.

A study of sweeping soaking time while holding nitridation temperature constant was done. At a temperature of 1200°C, there is near full conversion of γ-Al_2O_3 to aluminum nitride, with a slight the (220) peak, at 46°, γ-peak. Also, at this temperature, based on SEM imaging, the grain size of the powder shows no significant growth. At 1200°C, there were experiments where different hold times of the alumina powder, ranging from 1 hour to 24 hours. Based on XRD analysis, the longer the hold time of the sample the more nitrided it becomes. In Figure 4.2.5, the (220) at 46°, γ-peak disappears as the hold time increases.

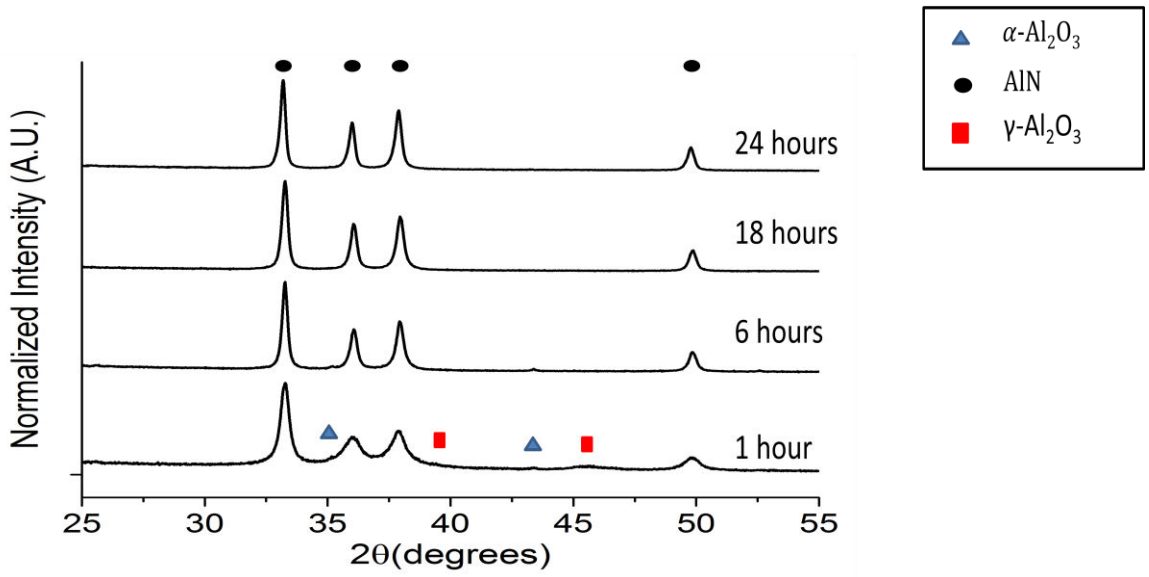

Figure 4.2.5. XRD patterns of γ-Al_2O_3 powders nitrided at 1200°C and held at different times.

Also, the width of the peaks decreases as the hold time increases, indicating that the grains size of the powder is increases. In order to get a visual representation on how the grains were developing in size, SEM images were taken. In Figure 4.2.6., there is a trend confirming that as the hold time is increased the grains slightly grow.

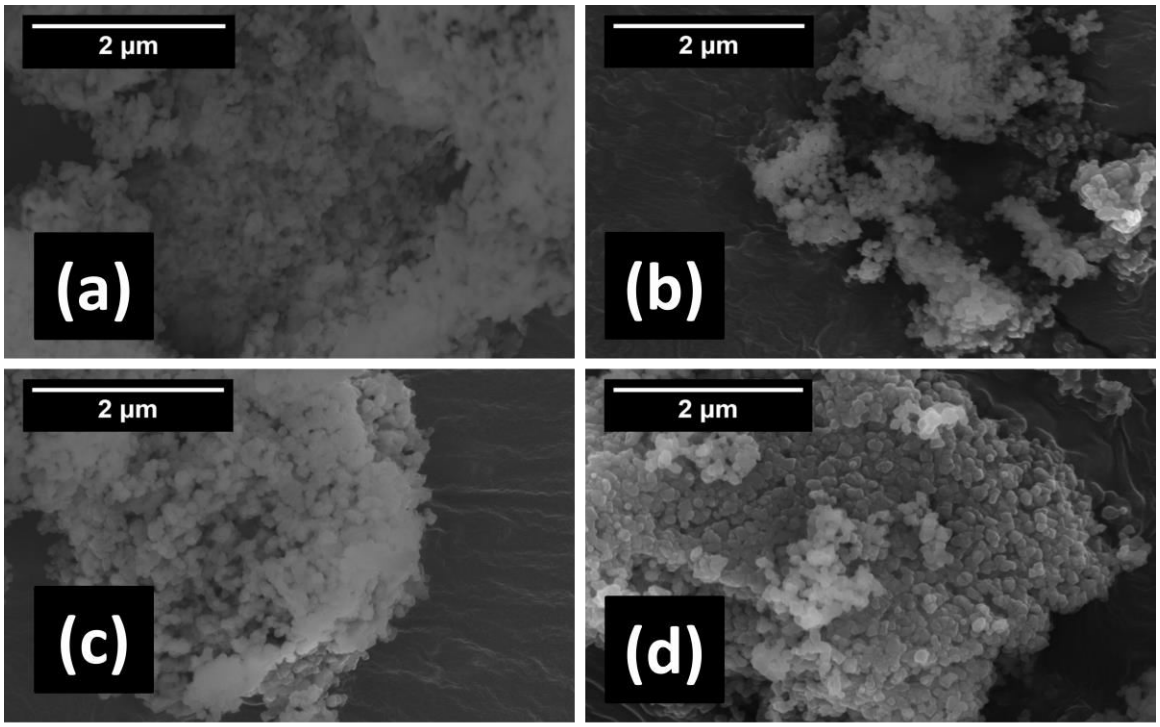

Figure 4.2.6. SEM images of powders processed at different holding times in the tube furnace (a) 1 hour (b) 6 hours (c) 18 hours and (d) 24 hours, at 1200°C each.

Figure 4.2.7 shows the effect of tube furnace processing temperatures on the grain size of aluminum nitride, measured by SEM. Each of the powders were processed for 1 hour each. At 1100°C, there is an approximate increase of double in terms of grain size from the starting commerical γ-Al_2O_3. As the temperature increases to 1300°C and

1400°C, there is a significant increase in grain size approximately around 110 and 200 nm, respectively. While, the conversion to aluminum nitride is guranteed at these temperatures, the powder has grown too large for futher processin g in CAPAD to be considered nanocrystalline.

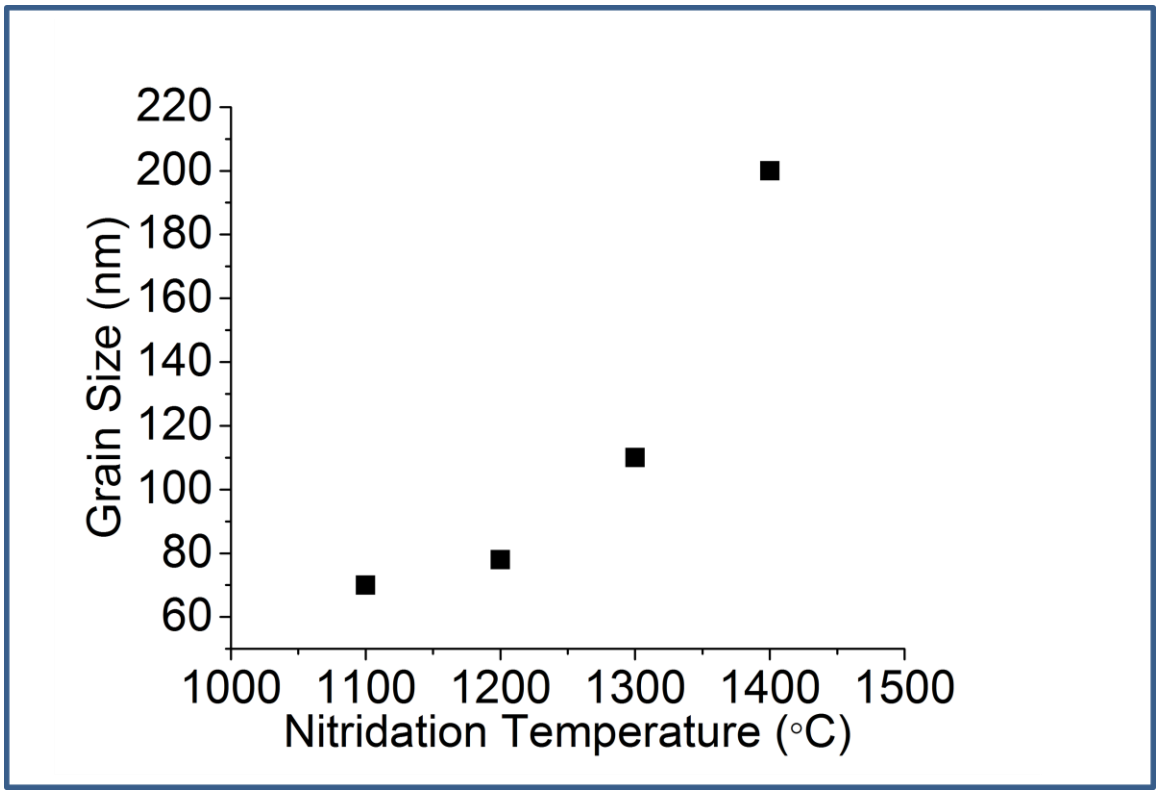

Figure 4.2.7. Effect of tube furnace processing temperature on grain size. Powders were processed for 1 hour.

At 1200°C, there is a small amount of γ-Al_2O_3 when processed for 1 hour. However, when the processing time is increased to 6 hours, the intensity of (220) at 46°, γ-peak has decreases. When the processing time is held for 18 hours, there are no traces of γ-Al_2O_3 or any other phase, detectable by XRD. The processing parameter of

choicewould then be 1200°C powder held for 18 hours for CAPAD processing . With those parameters, the y-Al2O3 is fully converted and the grain size is still relatively small. Figure 4.2.8., shows grain size development as the processing time increases from 1, 6, 18 to 24 hours.

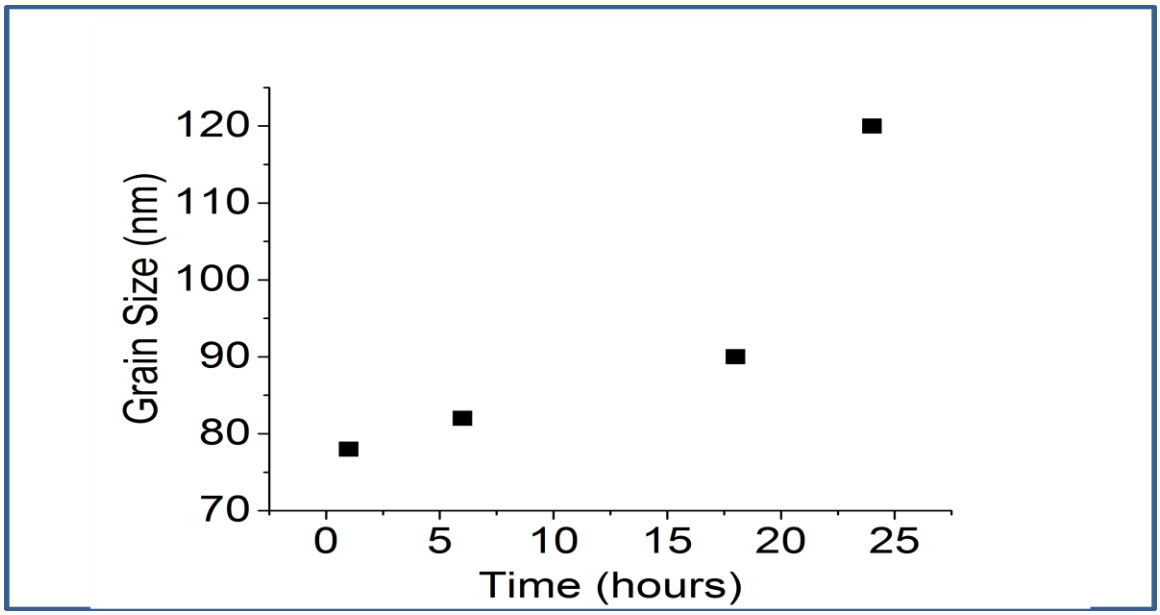

Figure 4.2.8. Effect of time on grain size of aluminum nitride. Powders processed at 1200°C.

For each of these processing times, the temperature was held at 1200°C, and the relationship between grain size and time looks to follow a exponential curve.

4.3 Nanocrystalline Aluminum Nitride Bulk from CAPAD Processing

The synthesized powders from the tube furnace were processed under CAPAD to yield a 3D bulk material. The morphology and composition of AlN is discussed. The powder used in CAPAD processing was processed in the tube furnace for 18hours at 1200C at position 10. The powder was then processed in CAPAD at a pressure of 105

MPa, temperature ranges of 1100-1600°C and held at these temperatures for 10 minutes. The bulk samples show a range of grain size growth, as shown in figure 4.3.1, as processing temperatures increases. At 1100°C, there are many pores present in the

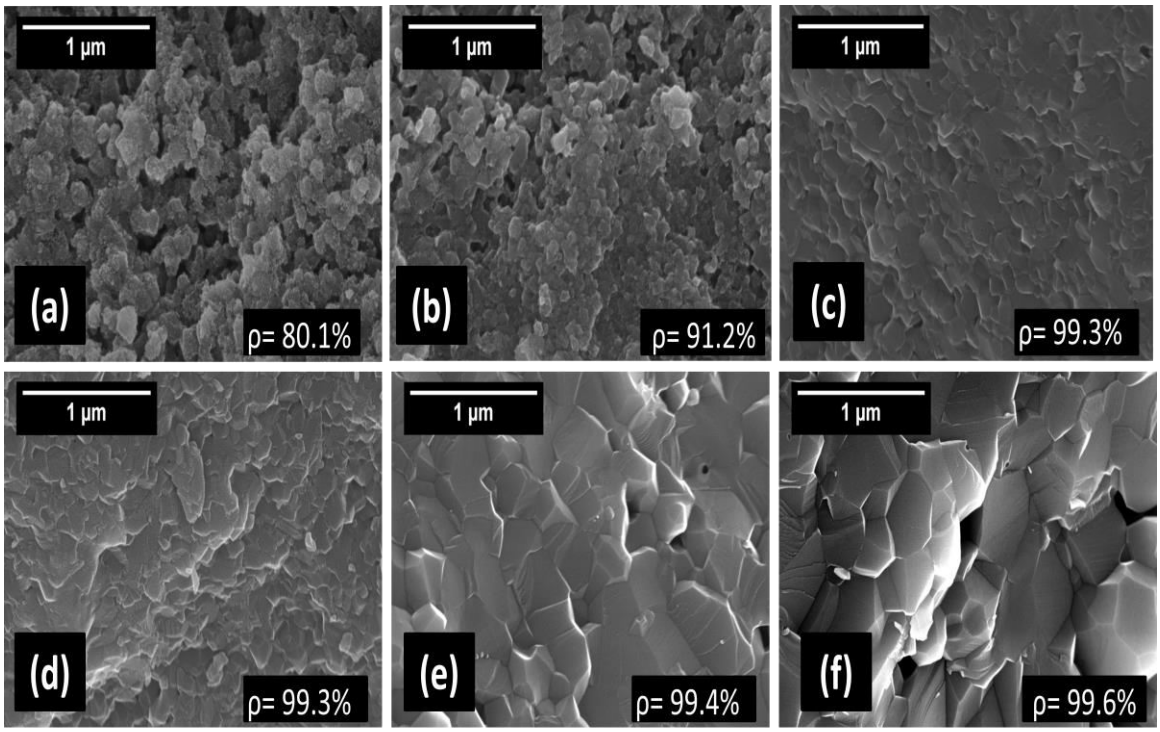

Figure 4.3.1. SEM images describing the grain size development of the aluminum nitride bulk as CAPAD processing temperature increases from (a) at 1100°C, (b) 1200°C, (c) 1300°C (d) 1400°C, (e) 1500°C and (f) 1600°C.

material and as the temperature increases the amount and size of the pores decreases. At 1300C there is a significant decrease in the amount of pores in the material having a relative density of 98.5% ,calculated using the Arcimedes principle:

$$\frac{density\ of\ object}{density\ of\ fluid} = \frac{weight}{weight\ of\ displaced\ fluid} \qquad (4.3.1)$$

where the fluid used was ultra high pure water. Every bulk sample's density was measured using Archimedes principle, and a plot of density in relation to CAPAD processing temperature is shown in figure 4.3.2. It is well known that as temperature

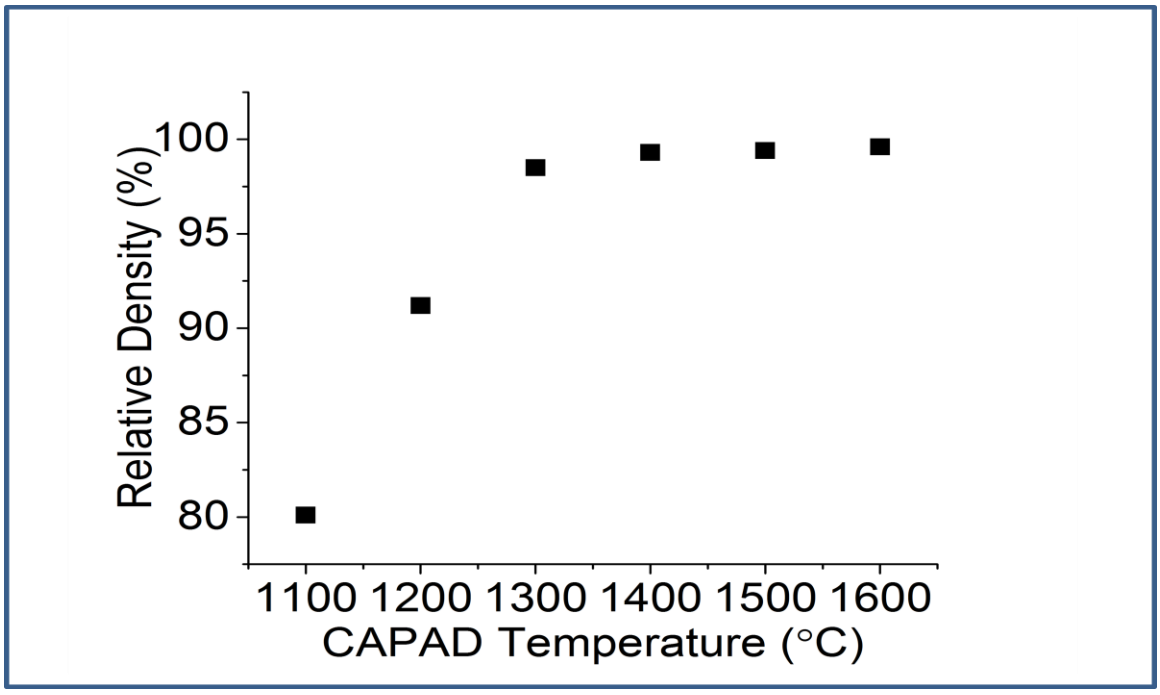

Figure 4.3.2. Effect of CAPAD processing temperature on bulk density.

increases when trying to obtain a dense sample, the density will increase to an extent. The reason behind this is, mass transfer causes the fillng of the voids and grain growth. As the grains grow, the porosity, for the most part, shrink and disappear. As the grains grow further reduction in the surface energy is achieved by reducing the total area of grain boundary. The boundary between one grain and its neighbor is a defect in the crystal structure and so it is associated with a certain amount of energy. As a result, there is a thermodynamic driving force for the total area of boundary to be reduced. If the grain

size increases, accompanied by a reduction in the actual number of grains per volume, then the total area of grain boundary will be reduced [22].

This is seen when transitioning at temperatures of 1200°C to 1300°C. At 1400°C, there isn't an significant increase in the relative density of the bulk in comparison to 1300°C and even less so at 1500°C and 1600°C. Reaching relative densities 99.4% and 99.6%, at 1500°C and 1600°C, respectively. At the higher temperatures, the majority of the pores have disappeared and only grains growing into one another remains.

XRD analysis of aluminum nitride 3D bulk material was run as the temperature was swept. Analysis reveals that when processing in CAPAD conditions, the material becomes a two phase system, being that of AlN and aluminum oxynitride, AlON. The AlON present in the material is that of a defect structure, Al9O3N7, and not the common spinel structure. The AlON in the material, doesn't start to show in XRD until we reach

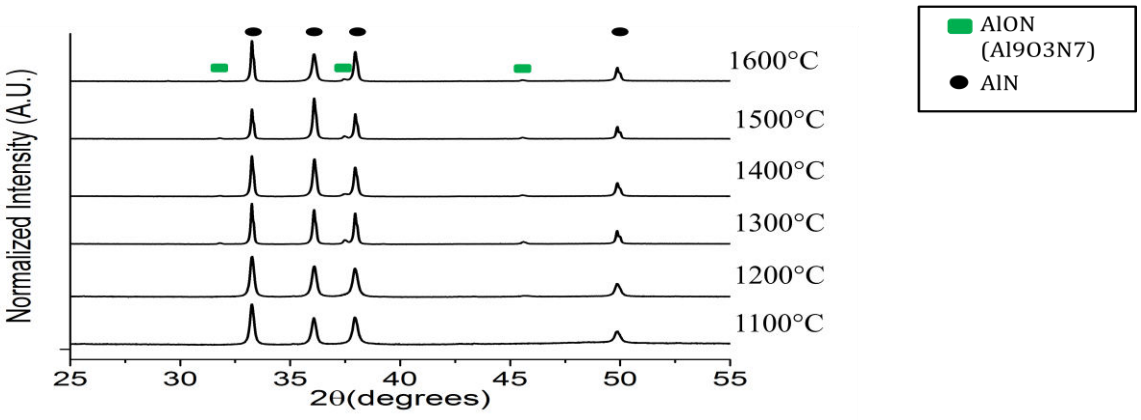

Figure 4.3.3. XRD analysis of aluminum nitride 3D bulk material as temperature is swept.

temperatures of 1300°C and higher. At 1100°C and 1200°C, the corresponding AlON peaks, (101) and (013) at 33.7° and 37.4°, aren't present. The appearance of AlON in our system raises questions about the purity of our samples or the oxygen "free" environment we are preparing our samples in. The impurity in our samples will be discussed in a later section.

Through all the CAPAD processing, analysis of the grain size as afunction of temperature was obtained. As shown in Figure 4.3.4, the grain size of bulk aluminum nitride increases as the processing temperature is increases. At 1100°C the grain size of the material is below 100 nm and at 1600°C the grains have grown so large they are in the sub-micron region, >300 nm. The relationship between grain size and temperature follows an exponential trend. If the processing temperatures were to increase even higher the grain size would grow at a fast rate. Figures 4.3.2, and 4.3.4, show the

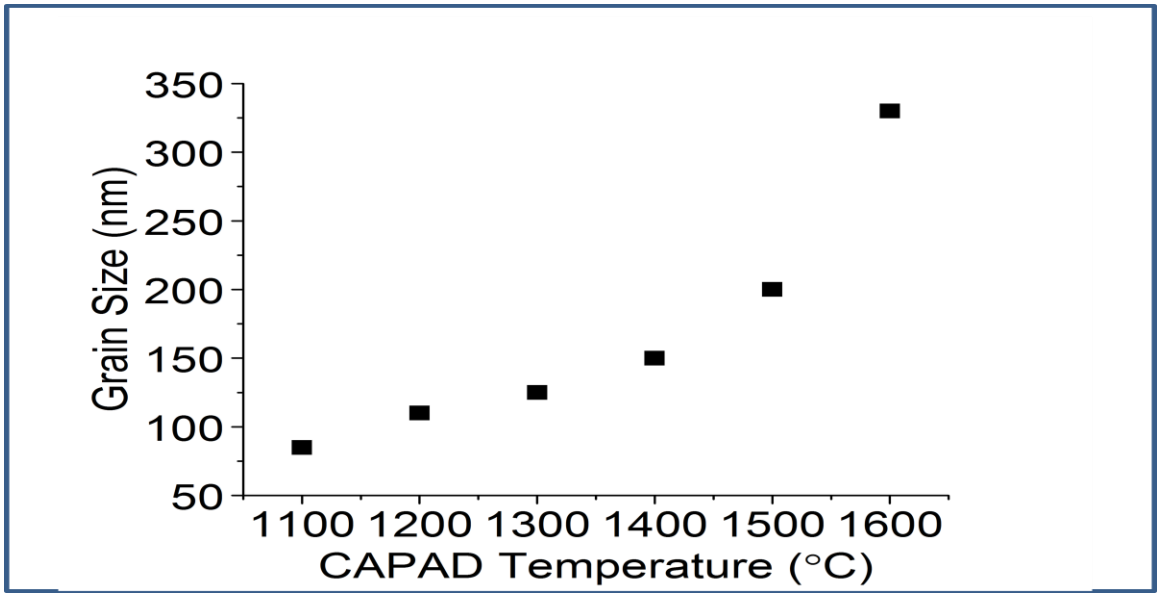

Figure 4.3.4. Effect of CAPAD processing temperature on grain size of bulk aluminum nitride.

relationship between CAPAD processing temperatures, relative density and grain size. Both grain size and density of the aluminum nitride bulk increase as the CAPAD processing temperature increases.

Work done by one of our colleagues, where commercially available Tokuyama powders were processed under similar CAPAD conditions are shown in figure 4.3.5. [23]. The Tokuyama powder has an initial grain size of 1-2 μm with a purity of 97%.

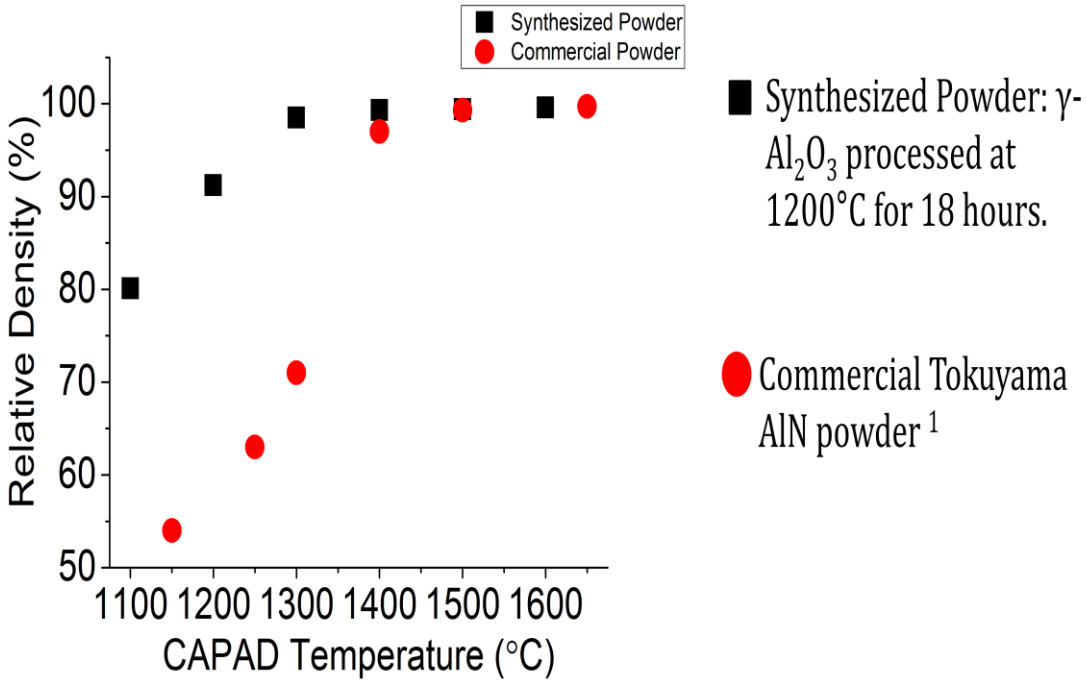

Figure 4.3.5. Relative density vs processing temperature for aluminum nitride bulk samples, where powders used were synthesized from nitriding γ-Al_2O_3 at 1200°C for 18 hours and commercial Tokuyama powder.

When comparing the densities of the bulk aluminum nitride processed from the synthesized and commerical powder, there is a difference. The bulk that was processed from the syntheiszed powder was able to achieve a higher dense sample at lower temperatures. The bulk sample processed with the commerical powder, required a higher temperature to achieve the same density. When both powders were processed at 1200°C, there is a density difference of approximately 30%. This difference in density is attributed to the nature of the processes powder. Since the synthesized powder has grains with the size of ~90 nm, they are more crystallites available per unit volume, so the green body density of the compact will be high. This is represented a schematic in Figure 4.3.6.

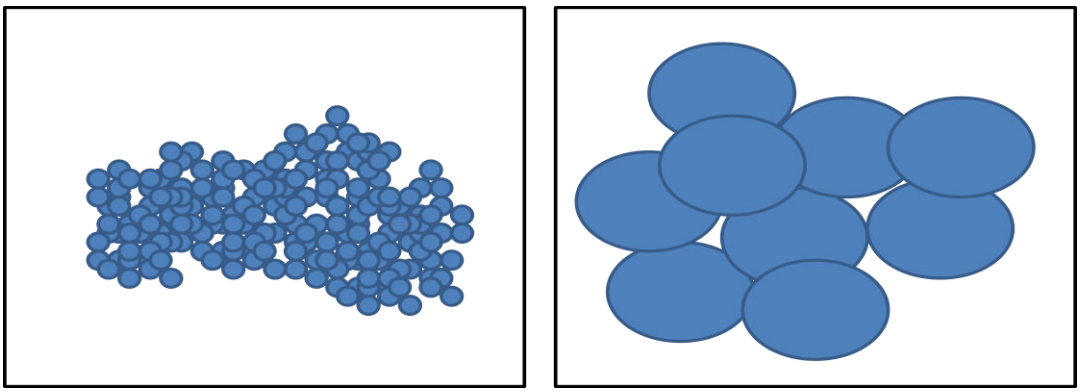

Figure 4.3.6. Schematic repressenting the difference in powder compaction between small and large crystallites.

When the powder is beginning the densification process, less energy (temperature) will be required for the nanosized powder to grow its grain and fill any porosity. The commerical Tokuyama, with grain size of 1-2 um, would require more energy to grow its grains and . The density of the bulk will increase as the pores shrink or decrease.

When comparing between synthesized powder and the commercial powder, the difference in density is evident. However, when comparing the densities between powders processed in different conditions, the difference is less apparent numerically. In Figure 4.3.7, powders processed at lower temperatures and time, the powder with smaller grains, reveal a higher density although very slightly. The real difference lies visually.

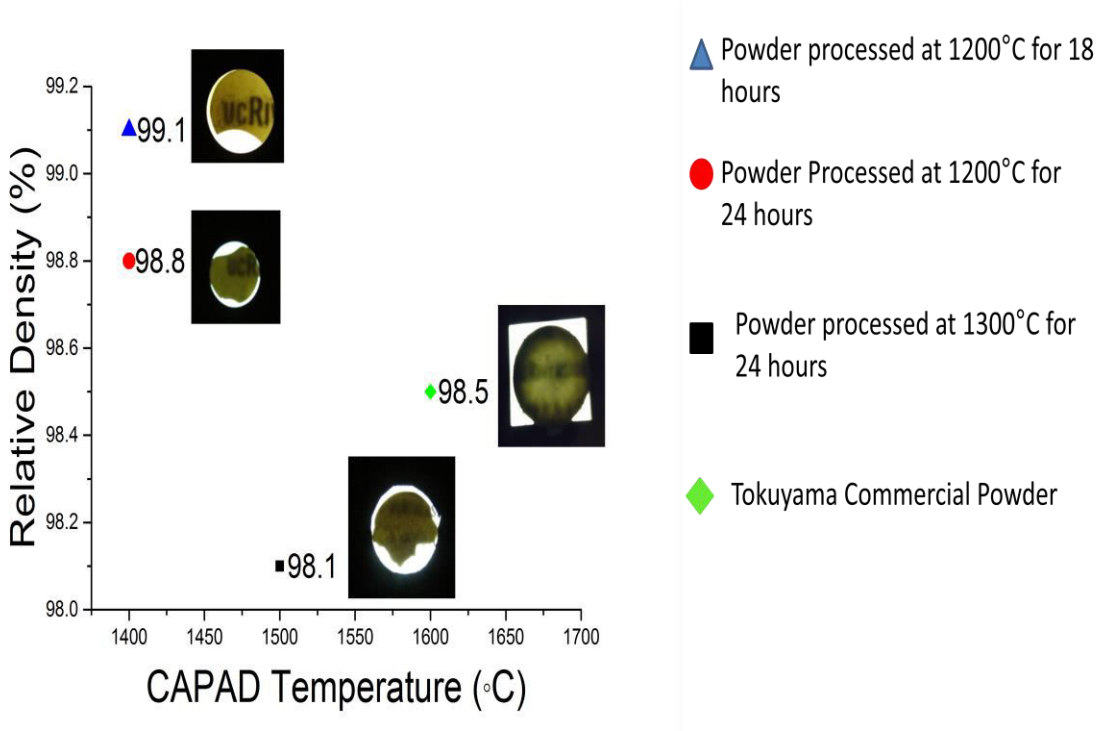

Figure 4.3.7. Plot of relative density vs CAPAD processing temperature

The bulk samples processed with the finer powders are translucent. When we see the transluscency of the bulk aluminum nitride samples, there is a visual representation on the density of the samples, or lack of pores. For this reason, achieving high density is crucial. This would not be possible with processing the commercial powder, the grain size, already micron-sized, would grow too large if higher processing temperatures are

required to achieve high density. The entire purpose was to synthesize nanocrystalline bulk aluminum nitride, something not possible with the use of commerical powder.This would set us futher from our goal of having nanocrystalline bulk aluminum nitride.

Another major proponent of our goal was to have single phase aluminum nitride, having any second phase might be detrimental to the properties of aluminum nitride.

4.4 Impurity in Aluminum Nitride

As mentioned earlier, there is an impurtiy in our bulk aluminum nitride samples. The impurity in this case being oxygen, which will form AlON. When looking at figure 4.4.1, there are multiple small AlON peaks with the majority of the material

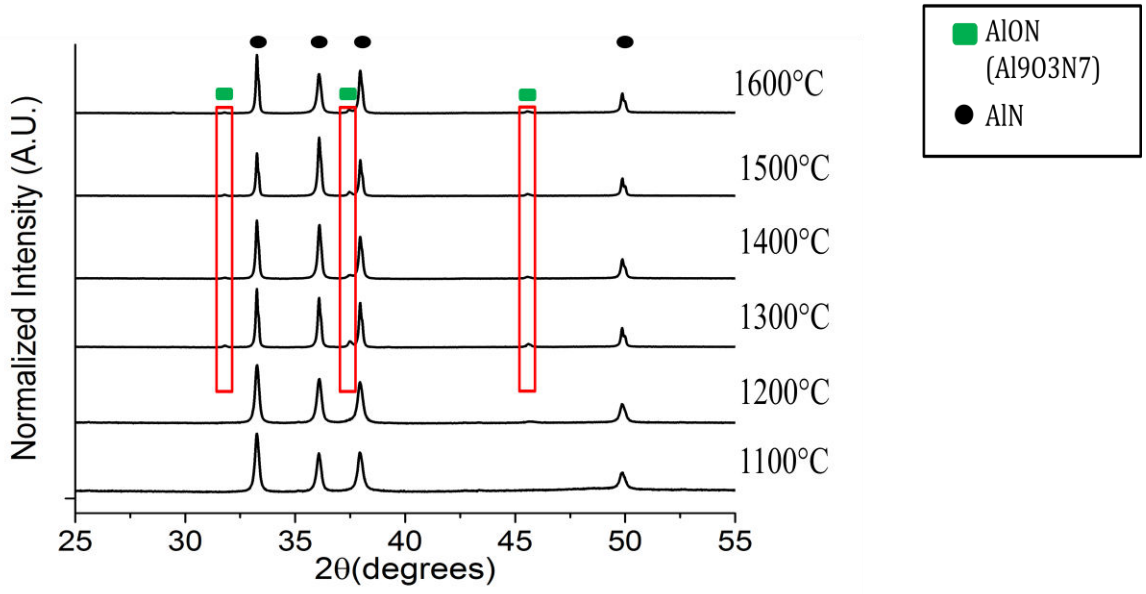

Figure 4.4.1. XRD Analysis of bulk aluminum nitride with the presence of AlON shown in the red boxes.

being aluminum nitride. As previously stated the corresponding AlON peaks, (101), (013) and (036) at 33.7°, 37.4° and 45.3°. Although, the intensity of the AlON peak is small, it is still detectable byXRD meaning that the concentration of AlON is >5%. At higher temperatures, oxygen will start to react with the aluminum nitride to form a solid solution. As the temperature increases even more, AlON will begin to precipitate out and the concentration of AlON increases. This is the reason why we see AlON peaks forming in XRD.

This is a problem is because aluminum nitride's thermal conductivity depends on the purity of material, with a value between 70-270 W/(m*K), while AlON has a thermal conductivity of 10 W/(m*K) [24], at room temperature. Having a mixture between two phases with a large difference in thermal conductivity values will greatly affect the overall thermal conductivty of the material.

Sources of Impurity

The distribution of oxygen impurities in aluminum nitride is a function of the powder's synthesis method. There are two sources of oxygen impurity in our processing methods. The first being oxygen remaining in the lattice. For powders prepare by the reduction of aluminum oxide, oxygen remains from incomplete conversion of Al_2O_3. This residual oxygen is identified as lattice oxygen [25]. The second source of powder oxygen is from the exposure of aluminum nitride to air. Because aluminum nitride has a strong affinity to bond with oxygen, it will readily attempt to bond to any oxygen present. The oxygen will then form a surface layer of rich oxygen or an oxide layer on the surface of

aluminum nitride powder. At any time there is a chance for aluminum nitride to be exposed to air, there is a rich for oxygen contamination [9, 26]. A schematic of this is shown in figure 4.4.2.

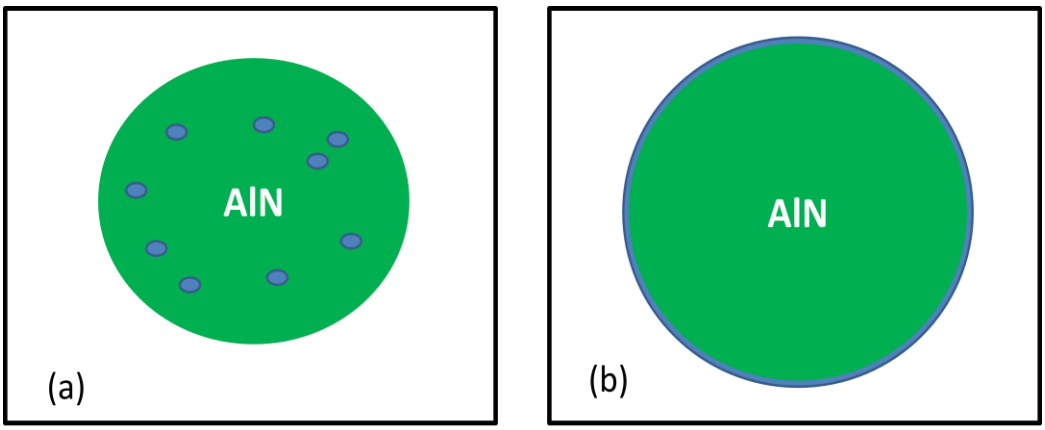

Figure 4.4.2. A representation of the different types of oxygen impurities in aluminum nitride powders. The oxygen impurity is represented by the blue, with (a) lattice oxygen remaining from incomplete conversion and (b) surface oxygen from exposure to air.

The amount of oxygen concnetration and location of the oxygen is important to understanding how the properties of aluminum nitride will be affected. However, the location of the oxygen in the powders is unknown and the concentration oxygen cannot be determined from XRD analysis alone, which is the only analysis we have. If the location of oxygen impurity was heterogeneously disbursed in the material, there might not be a big effect on the thermal properties since the oxygen concentration would be segregated. Further analysis on these samples is required to better understand where and the amount of oxygen there is.

Chapter 5 Summary and Conclusion

A synthesis method of aluminum nitride was performed ofr the purpose of creating nanocrystalline single phase aluminum nitride powder. The aluminum nitride powder was synthesized using the reduction and nitridation of commercial γ-Al_2O_3 through a tube furnace by flowing ammonia. We were able to obtain nano-sized aluminum nitride powder, sizes ranging from 70 to 200 nm, through this processing method. By controlling the processing condition in the tube furnace such as, temperature and time, the powder's morphology is reatined after nitridation. These powders were consolidated through CAPAD processing and sub micron grains were achieved, 85-330 nm. The synthesized powders when processed in CAPAD was able to achieve an overall higher density than that of the commercial Tokuyama powder under similar conditions, although not single phase. The bulk samples that derived from the synthesized powders consisted of a mixture of two phases, aluminum nitride (the majority) and AlON. By being able to effectively optimize the processing parameters in powder and bulk form, dense nanocrystalline aluimum nitride can be synthesized.

References

[1] I. Levin, D. Brandon, "*Metastable Alumina Polymorphs: Crystal Structures and Transition Sequences,"* J. Am. Ceram. Soc., vol. 81, no. 8, pp. 1995-2012, Jan. 2005.

[2] M. Ramisety, S. Sastri, U. Kashalikar, *"Manufacturing of Aluminum Nitride for Advanced Applications,"* Am. Ceram. Soc. Bulletin, vol. 93, no. 6, pp. 28-31, 2012

[3] A. Franco Junior, D. J. Shanafield, *"Thermal Conductivity of polycrystalline aluminum nitride (AlN) ceramics,"* Ceramica, vol. 50, pp. 247-253, 2004.

[4] K. Momma and F. Izumi, "VESTA 3 for three-dimensional visualization of crystal, volumetric and morphology data," J. Appl. Crystallogr., 44, 1272-1276 (2011).

[5] R.W. Rice, C.C. Wu, F. Borchelt, "*Hardness-Grain-Size Relations in Ceramics,"* J. Am. Ceram. Soc., vol. 77, no. 10, pp. 2539-53, 1994.

[6] X. Liu, F. Yuan, Y. Wei, "*Grain size effect on the hardness of nanocrystal measured by the nanosized indenter,"* App. Surf. Sci., vol. 279, pp. 159-166, 2013.

[7] K. M. Taylor, C. Lenie, "*Some Properties of Aluminum Nitride"* Journal of Electrochemical Soc., 1960, pp. 308-314.

[8] A. Franco Junior, D. J. Shanafield, *"Thermal Conductivity of polycrystalline aluminum nitride (AlN) ceramics,"* Ceramica, vol. 50 no.315, pp. 247-253, 2004.

[9] G. A. Slack, R. A. Tanzilii, R. O. Pohl, J. W. Vander Sonde, J. Phys. Chem. Solids 1987, 48, 641.

[10] J. H. Kong, M. Okumiya, Y. Tsunekawa, S.G. Kim, M. Yoshida, "*AlN and intermetallic compound layers formed between alumina and austenitic stainless stee using barrel nitriding,"* Prog.Org. Coat., vol. 76, pp. 1841-1845, 2013.

[11] T. Yamakawa, J. Tatami, K. Komeya, T. Meguro, *"Synthesis of AlN powder from Al(OH)3 by reduction–nitridation in a mixture of NH3–C3H8 gas"* J. Euro. Ceram. Soc, 26 pp. 2413–2418. 2005.

[12] Kroke, E., Loeffler, L., Lange, F. F. and Riedel, R., "*Aluminum nitride prepared by nitridation of aluminum oxide precursors".* J. Am. Ceram. Soc., 2002, 85, 3117–3119.

[13] C. Wang, S. Chen, "*Factors influencing particle agglomeration during solid-state sintering,"* Acta. Mech. Sin., vol. 28, no.3, pp. 711-719, 2012.

[14] J. E. Garay, "Current-Activated, Pressure-Assisted Densification of Materials," Annu. Rev. Mater. Res., vol. 40, no. 1, pp. 445–468, Jun. 2010.

[15] R. A. Swalin, *Thermodynamics of Solids*, 2nd ed. Wiley-VCH; 2 editions (December 15, 1972), 1972, p. 400.

[16] L. C. Jonghe, M. N. Rahaman, *"Sintering of Ceramics,"* Handbook of Advanced Ceramics, 2003.

[17] J. Wiley, *Fundamentals of Materials Science and Engineering An Interactive*.

[18] A. Patterson, *"The Scherrer Formula for X-Ray Particle Size Determination," Phys. Rev.*, vol. 56, no. 10, pp. 978–982, Nov. 1939.

[19] V. Kazmiruk, *Scanning Electron Microscopy*. Croatia, 2012, p. 830.

[20] R. A. Llewellyn and P. A. Tipler, *Modern Physics*, 5th ed. New York, 2008, p. 673.

[21] C. Ronda, Luminescence From Theory to Applications (Wiley-VCH, New York, 2008)

[22] F. J. Humphreys and M. Hatherly (1995); *Recrystallization and related annealing phenomena*, Elsevie

[23] A. T. Wieg,1 Y. Kodera,1 Z. Wang,1 T. Imai,2 C. Dames,3 and J. E. Garay. *Visible photoluminescence in polycrystalline terbium doped aluminum nitride (Tb:AlN) ceramics with high thermal conductivity.* University of California, Riverside, California. Ryukoku University, Ohtsu, Japan. University of California, Berkeley, California. APPLIED PHYSICS LETTERS 101, 111903 (2012).

[24] ALON Optical Ceramic. Surmet Engineering. 2015.

[25] T. A Guiton, J. E. Volmering, K. K. Killinger, Mat. Res. Soc. Symp. Proc. **271** (1992) 851.

[26] G. A Slack, J. Phys. Chem. Solids **34** (1973) 321-335.